KfK 4286
Oktober 1987

Probabilistic Analysis of Crack Containing Structures with the PARIS Code

A. Brückner-Foit
Institut für Material- und Festkörperforschung

Kernforschungszentrum Karlsruhe

KERNFORSCHUNGSZENTRUM KARLSRUHE

Institut für Material- und Festkörperforschung

KfK 4286

Probabilistic Analysis of Crack Containing Structures with the PARIS Code

A. Brückner-Foit

KERNFORSCHUNGSZENTRUM KARLSRUHE GMBH, KARLSRUHE

Kernforschungszentrum Karlsruhe GmbH
Postfach 3640, 7500 Karlsruhe 1

ISSN 0303-4003

Abstract

The basic features of the PARIS code which has been developed for the calculation of failure probabilities of crack containing structures are explained. An important issue in the reliability analysis of cracked components is the probabilistic leak-before-break behavior. Formulae for the leak and break probabilities are derived and it is shown how a leak detection system influences the results. An example taken from nuclear applications illustrates the details of the probabilistic leak-before-break analysis.

Probabilistische Analyse rißbehafteter Strukturen mit dem Progamm PARIS

Die Grundzüge des Programms PARIS, das zur Berechnung der Ausfallwahrscheinlichkeiten rißbehafteter Strukturen entwickelt wurde, werden erläutert. Ein wichtiger Punkt in der Zuverlässigkeitsbeurteilung von Komponenten mit Rissen ist die probabilistische Leck-vor-Bruch-Analyse. Es werden Formeln für die Leck- und die Bruchwahrscheinlichkeiten abgeleitet, und es wird gezeigt, wie ein Leckentdeckungssystem die Ergebnisse beeinflußt. Ein Beispiel aus der Kerntechnik veranschaulicht die Einzelheiten der probabilistischen Leck-vor-Bruch-Analyse.

Table of Contents

Introduction

Probabilistic fracture mechanics (PFM) has been developed in recent years in order to estimate the reliability of components containing cracks (for reviews see /1/ - /3/). A fracture mechanical analysis provides failure criteria applicable to each individual crack in a given component. The failure probability is then defined as the probability of finding combinations of crack sizes, loads and material parameters such that the applied stress exceeds the critical stress determined by the failure criterion. A survey of the state-of-the-art and of applications of PFM in the aircraft and in the nuclear industry is given in /4/.

The failure probability can be determined analytically or by straightforward numerical integration in simplified cases only /5/. Monte Carlo simulation including variance reducing techniques turns out to be a powerful tool for the numerical analysis of general PFM problems. Several codes using Monte Carlo methods have been developed for applications in the nuclear industry. The OCTAVIA-/6/, VISA-/7/, OCA-P-/8/ and COVASTOL-codes /9/ have been devised for the PFM analysis of reactor pressure vessels. Special emphasis is put on the assessment of radiation embrittlement and of pressurized thermal shocks. The PRAISE-code /10/ has been designed for calculating the leak and break probabilities for pipes in the primary coolant loop of a PWR. ISPUD /11/ is a Monte Carlo program using variance reducing techniques for which the fracture mechanical model has to be provided by the user.

The development of the PARIS-code (PARIS is an acronym for "Probabilistische Analyse rißbehafteter Strukturen" = probabilistic analysis of cracked components) described in this report was motivated mainly by the idea that a general code should be available with which PFM analyses of a variety of components can be performed without any major programming effort. Additionally, it was felt that the highly sophisticated variance reducing techniques (for an overview, see e.g. /12/) should be standardized as in the ISPUD-code in order to avoid systematic errors occurring inadvertedly in the simple-minded application of these techniques. In the first section of this report, the basic features of PFM analyses using Monte Carlo simulation are sketched. Variance reduction by importance sampling is introduced. The second section contains analytic expressions for the failure probability of crack containing components including the effect of fatigue crack growth, in-service inspections, leak-before-break-behavior, leak detection systems, etc. These formulae form the theoretical background of the code. Additionally, an iterative procedure based on Spanier's algorithm /13/ is described which enables the user to specify suitable importance sampling distributions such that rapid convergence of the simulation is ensured. In the third section the detailed structure of the code is described at some length. The fourth section contains an example typical of nuclear applications of PFM /14/ in order to illustrate some of the characteristics of the code.

1. Monte Carlo Simulation in Probabilistic Fracture Mechanics

1.1 Basic Ideas

If all the cracks contained in a component are independent of each other, its failure probability can be expressed as

$$Q = 1 - \exp(- M \cdot Q_1) \quad . \tag{1.1}$$

where M is the average number of cracks per component and Q_1 is the failure probability provided that one and only one crack is present. Q_1 is given by

$$Q_1 = \int_{-\infty}^{+\infty} f(x_1) \ldots \int_{-\infty}^{+\infty} f(x_k) \int_{a_c(x_1,\ldots,x_k)}^{t} f(a)\, da\, dx_k \ldots dx_1 \tag{1.2}$$

$x_1,\ldots,x_k$ are input quantities such as fracture toughness, flow stress, applied stress and crack length influencing the critical crack depth a_c; a denotes the crack depth, $f(x_i)$ the probability density assigned to x_i, and t the wall thickness.

The conditional probability Q_1 is expected to take a very small value for components of high reliability such as nuclear structures and has to be determined numerically by solving the multi-dimensional integral eqn. (1.2). This can be performed either by conventional numerical integration or by Monte Carlo simulation, the latter being more favorable in case of higher dimensions and complicated formulae for a_c.

Direct Monte Carlo simulation is equivalent to performing numerical experiments. A crack of fixed crack depth is selected from a sample of cracks generated according to the probability distribution F(a). This corresponds to considering a sample of nuclear components each containing one crack of the depth selected. Each particular crack is compared with a critical crack depth resulting from specific values of x_i of the corresponding samples. If a is less than a_c, the numerical experiment does not lead to a failure of the component under consideration ("miss"), whereas cases with $a > a_c$ are counted as "hits." After n simulation runs, the failure probability of the real component is estimated to be

$$Q_D = \frac{\text{number of hits}}{\text{number of trials}} \tag{1.3}$$

The standard error of this estimator is equal to

$$s_{DE} = \sqrt{\frac{Q_D\,(1 - Q_D)}{n}} \tag{1.4}$$

The simulation method has two clear disadvantages:

i) A compromise has to be made between calculation speed and accuracy. For a typical failure probability of the order of 10^{-7}, about 10^7 simulation runs have to be performed in order to obtain an average of one hit.

ii) The numerical results will contain inherent statistical fluctuations which will vanish only as $\sqrt{n}$.

However, direct simulation has certain advantages, because complicating effects such as fatigue crack growth and elasto-plastic failure criteria can be introduced directly into the simulation procedure, which is impossible in numerical integration. A fair compromise seems to be to perform as many analytical integrations as possible and to use variance reducing techniques to solve problems i) and ii).

1.2 Importance Sampling

The fundamental numerical problem to be solved in PFM is to compute the integral

$$Q_1 = \int_0^{\infty} f\,(K_{Ic}) \int_{a_c}^{t} f\,(a)\, da\, dK_{Ic} \tag{1.5}$$

or, equivalently,

$$Q_1 = \int_0^{t} f\,(a) \int_0^{K(a)} f\,(K_{Ic})\, dK_{Ic}\, da \tag{1.6}$$

where a is the crack depth, K_{Ic} the fracture toughness, t the wall thickness, K the stress intensity factor, and $f(\cdot)$ the respective normalized probability density. An analytical integration leads to

$$Q_1 = \int_0^{t} f\,(a)\; h\,(a)\; da \tag{1.7}$$

where

$$h(a) = F(K_{Ic} = K(a))$$

and $F(K_{Ic})$ denotes the probability distribution of K_{Ic}. In case of constant K_{Ic}, h(a) is a step function defined as

$$h(a) = \begin{cases} 1 & \text{for } K(a) \geq K_{Ic} \\ 0 & \text{for } K(a) < K_{Ic} \end{cases} \tag{1.8}$$

It is clear that in the one-dimensional case of Eq. (1.7), Q_1 can be evaluated much more efficiently by conventional numerical means than by Monte Carlo methods, but let us consider eqn. (1.7) as an illustrative example. In a Monte Carlo simulation for the calculation of Q_1 random numbers are generated representing the random crack size a and the random fracture toughness K_{Ic} $K(a) > K_{Ic}$ corresponds to a "hit" in eqn. (1.3).

An alternative method of calculating Q_1 is to interpret eqn. (1.7) as an expectation value of h(a) with respect to the distribution F(a). Crude Monte Carlo amounts to computing

$$Q_C = \frac{1}{n} \sum_{i=1}^{n} h(a_i) \tag{1.9}$$

for a sample of size n generated with a random number generator according to the distribution F(a). This means that the expectation value, eqn. (1.7) is estimated by the corresponding arithmetic mean. The variance of the estimator is given by

$$s_C{}^2 = \frac{1}{n-1} \sum_{i=1}^{n} (h(a_i) - Q_C)^2 \tag{1.10}$$

wherefrom the standard error can be determined:

$$s_{CE} = \sqrt{\frac{s_C{}^2}{n}} \tag{1.11}$$

Several methods are available for further reducing the error of the simulation /12/. Importance sampling is used in the PARIS code which amounts to biasing the simulation by the use of another distribution so that the part of the integrand in eqn. (1.7) that makes the highest contribution to the integral is emphasized in the sampling. To avoid introducing a bias in the final result, corrections are made at the end. Let us represent Q_1 in the following way to illustrate the method:

$$Q_1 = \int_0^t h(a) \cdot \frac{f(a)}{f_I(a)} \cdot f_I(a)\, da = \int_0^t h(a) \cdot \frac{f(a)}{f_I(a)}\, dF_I(a) \tag{1.12}$$

where $f_I(a)$ is called the importance sampling density and its support includes that of f. Let $a_{I1},\ldots,a_{In}$ denote random observations from F_I. Then an unbiased estimate of Q_I is given by:

$$Q_I = \frac{1}{n} \sum_{i=1}^{n} h(a_{Ii}) \cdot \frac{f(a_{Ii})}{f_I(a_{Ii})} \tag{1.13}$$

The density f_I is to be chosen so that there is an abundance of observations in the region of large values of h(a) and so that the ratio $h(a_{Ii})\ f(a_{Ii})/f_I(a_{Ii})$ does not greatly fluctuate for the different values of a_{Ii}. If these requirements are fulfilled, the variance estimated

$$s_I^2 = \frac{1}{n-1} \cdot \sum_{i=1}^{n} \left[h(a_{Ii}) \cdot \frac{f(a_{Ii})}{f_I(a_{Ii})} - Q_I \right]^2 \tag{1.14}$$

will be much less than the variance of Crude Monte Carlo sampling given in eqn. (1.11). The corresponding standard error is given by

$$s_{IE} = \sqrt{\frac{s_I^2}{n}} \tag{1.15}$$

In general, a global optimum importance density is difficult to find. Spanier /13, 15/ developed an iterative procedure to locate the best choice within a single parameter family $f_I(a, \mu_I)$. For a particular $\mu_I = \mu_o$, the first term in the variance s_I^2 corresponding to the second moment is given by:

$$\frac{1}{n-1} \sum_{i=1}^{n} \left[\frac{h(a_{Ii})\ f(a_{Ii})}{f_I(a_{Ii}, \mu_0)} \right]^2 \tag{1.16}$$

where a_{Ii} is a random observation from $F_I(a, \mu_o)$. Formula (1.16) is an estimator of the integral

$$\int_0^t \left[\frac{h\,(a) \quad f\,(a)}{f_I\,(a,\,\mu_0)} \right]^2 dF_I\,(a,\,\mu_0) = \int_0^t \frac{(h\,(a) \quad f\,(a))^2}{f_I\,(a,\,\mu)}\, da \,\Big|_{\mu\,=\,\mu_0} \qquad (1.17)$$

If $\mu = \mu_1$ is selected, the right side of eqn. (1.17) becomes:

$$\int_0^t \frac{(h\,(a) \quad f\,(a))^2}{f_I\,(a,\,\mu_1)}\, da = \int_0^t \frac{(h\,(a) \quad f\,(a))^2}{f_I\,(a,\,\mu_1) \quad f_I\,(a,\,\mu_0)}\, dF_I\,(a,\,\mu_0) \qquad (1.18)$$

with the estimator

$$\frac{1}{n-1} \sum_{i=1}^{n} \frac{(h\,(a_{Ii}) \quad f\,(a_{Ii}))^2}{f_I\,(a_{Ii},\,\mu_1) \quad f_I\,(a_{Ii},\,\mu_0)} \qquad (1.19)$$

Thus, with one set of random numbers from $F_I(a,\ \mu_o)$, one estimates the second moment of other estimators arising from different choices of μ_I. Now, the value of μ_I is chosen that corresponds to the minimum variance estimate and a new batch of samples is generated. A few repetitions of this procedure usually lead to a near optimum choice of $f_I(a,\ \mu_I)$.

In realistic PFM problems, the failure probability depends on several random variables which means that variance reduction by importance sampling becomes much more complicated. The failure probability in a typical PFM problem is given by:

$$Q_1 = \int_0^\infty f\,(\sigma) \int_0^\infty f\,(K_{Ic}) \int_0^\infty f\,(\sigma_f) \int_0^1 f\,(a/c) \int_{a_c}^t f\,(a)\; da\; d\,(a/c)\; d\sigma_f\; dK_{Ic}\; d\sigma \qquad (1.20)$$

replacing the simple integral eqn. (1.5).

Generally speaking, there is no algorithm available to determine the optimum simulation strategy. Therefore, an iterative method relying on the basic ideas of Spanier's algorithm is used in the PARIS code (see Section 2.4).

2. General Features of the PARIS Code

2.1 Determination of Failure Probabilities

In the PARIS code failure probabilites are assumed to depend on the crack depth a, the depth-to-length ratio a/c, the fracture toughness K_{Ic}, the flow stress σ_f and the applied stress σ, each of which is an independent random variable with a probability distribution F(·). As the failure criteria contained in the code are more easily solved for the critical stress σ_c than for the critical crack depth a_c, the integral eqn. (1.20) is transformed to:

$$Q_1 = \int_0^\infty f\,(K_{Ic}) \int_0^\infty f\,(\sigma_f) \int_0^1 f\,(a/c) \int_0^t f\,(a) \int_{\sigma_c}^\infty f\,(\sigma)\; d\sigma\; da\; d\,(a/c)\; d\sigma_f\; dK_{Ic} \qquad (2.1)$$

Integrating the stress distribution leads to:

$$Q_1 = \int_0^\infty f\,(K_{Ic}) \int_0^\infty f\,(\sigma_f) \int_0^1 f\,(a/c) \int_0^t f\,(a) \cdot [1 - F\,(\sigma = \sigma_c)] \cdot da\; d\,(a/c)\; d\,\sigma_f\; dK_{Ic} \qquad (2.2)$$

where the integration domains of the random variables are independent of each other. Eqn. (2.2) is a four-dimensional generalization of eqn. (1.7) and can be evaluated numerically by using Monte Carlo simulation and variance reducing techniques.

In the PARIS code an importance sampling function f_I is introduced for each of the random variables, i.e. eqn. (2.2) is replaced by:

$$Q_1 = \int_0^\infty \frac{f\,(K_{Ic}}{f_I\,(K_{Ic})} \int_0^\infty \frac{f\,(\sigma_f)}{f_I\,(\sigma_f)} \int_0^1 \frac{f\,(a/c)}{f_I\,(a/c)} \int_0^t \frac{f\,(a)}{f_I\,(a)} \;[1 - F\,(\sigma = \sigma_c\;] \cdot$$

$$\cdot dF_I\,(a)\; dF_I\,(a/c)\; dF_I\,(\sigma_f)\; dF_I\,(K_{Ic}) \qquad (2.3)$$

(see eqn. (1.12)).

A sample of n random vectors $(x_1, x_2, \ldots, x_n)$ with $x_i = (a_i, (a/c)_i, (K_{Ic})_i, (\sigma_f)_i)$ is drawn from the joint probability distribution $F_I(a)\; F_I(a/c)\; F_I(K_{Ic})\; F_I(\sigma_f)$. As in the one-dimensional case (eqn. (1.13)), an unbiased estimator of Q_1 is given by:

$$Q_1 = \frac{1}{n} \sum_{i=1}^{n} \frac{[1-F(\sigma=\sigma_c)] \cdot f(a_{|i}) \; f((a/c)_{|i}) \; f((\sigma_f)_{|i}) \; f((K_{Ic})_{|i})}{f_I(a_{|i}) \; f_I((a/c)_{|i}) \; f((\sigma_f)_{|i}) \; f((K_{Ic})_{|i})} \tag{2.4}$$

The variance and the standard error are determined by generalizations of eqn. (1.14) and eqn. (1.15), respectively.

The PARIS code can also be used for problems involving fewer random variables than implied by eqn. (2.2). In this case, the distribution functions f_I and f have to be defined as constants leading to $f/f_I = 1$, and the appropriate constant value is assigned to the variable in question by the parameters of the distribution (see Section 3). If the applied stress is assumed to be constant, the probability distribution F(.) is replaced by a step function:

$$F(\sigma) = \begin{cases} 1 & \text{for } \sigma \geq \sigma_{appl} \\ 0 & \text{for } \sigma < \sigma_{appl} \end{cases} \tag{2.5}$$

For numerical convenience, the step function is replaced by a very narrow normal distribution, having a mean value equal to the specified constant and a coefficient of variation equal to 0.001.

In some cases of practical interest the applied stress varies within the component under consideration. Cracks can be found with equal probability at any location ($x_c < x < x_u$) throughout the component. Assuming that only the mean value depends on x and the variance remains fixed we can calculate $F(\sigma)$ as a function of the location. The square bracket in eqn. (2.2) has to be replaced by

$$\frac{1}{X_u - X_l} \cdot \int_{x_l}^{x_u} [1 - F(\sigma(x) = \sigma_c)] \, dx \tag{2.6}$$

in order to obtain the average failure probability for varying applied stresses.

2.2 Time Dependent Phenomena

The failure probabilities of structures containing cracks depend on time, if fatigue is included. In the PARIS code, stable crack growth due to prescribed cyclic loads is taken into consideration. No option for material degradation is included. For two-dimensional cracks, stable crack growth may lead to local instabilities and, subsequently, the formation of a stable through-wall crack (leak) or to global instabilities and catastrophic failure. Both possibilities are accounted for in the code. The maintenance of possibly flawed structures includes proof tests and non-destructive inspections. In the following sections, the basic formulae for the estimators of Q_1 are derived.

2.2.1 Stable Crack Growth

Within the framework of fracture mechanics stable crack growth caused by cyclic loads is described by a Paris type equation:

$$\frac{da}{dN} = C \cdot (\Delta K_A)^n$$

$$\frac{dc}{dN} = C \cdot (\Delta K_B)^n \qquad (2.7)$$

relating the change in crack length c and crack depth a per cycle to the variation of the stress intensity factor during one cycle. ΔK_A (ΔK_B) in turn depend on the actual crack configuration. Eqns. (2.7) can be considered as a system of ordinary differential equations from which $a(N, a_o, c_o)$ and $c(N, a_o, c_o)$ can be obtained by numerical integration using e.g. the Runge-Kutta method. a_o and c_o denote the initial crack depth and crack length.

In probabilistic fracture mechanics stable crack growth leads to a change in the distribution of crack size and shape according to the well-known formula /16/

$$f\,(a_0) \cdot f\,((a/c)_0) = f\,(a,\, a/c) \cdot \left| \frac{\partial\,(a,\, a/c)}{\partial\,(a_0,\, (a/c)_0)} \right| \qquad (2.8)$$

where

$$\left| \frac{\partial\,(a\,,\, a/c)}{\partial\,(a_0\,,\, (a/c)_0)} \right|$$

is the Jacobian of the functions $a = a(a_o,(a/c)_o,N)$ and $a/c = a/c(a_o, (a/c)_o,N)$ provided that there is a one-to-one correspondence between $(a, a/c)$ and $(a_o, (a/c)_o)$. Inserting eqn. (2.8) in eqn. (2.2) we obtain:

$$Q_1\,(N) = \int_0^\infty f\,(K_{Ic}) \int_0^\infty f\,(\sigma_f) \int_0^1 f\,((a/c)_0) \int_0^t f(a_0)\quad [1 - F\,(\sigma = \sigma_c\,(a,\,a/c))]\; da_0 d\,(a/c)_0 d\sigma_f\;dK_{Ic} \tag{2.9}$$

This means that stable crack growth can be accounted for by appropriately changing the value of the critical stress. Correspondingly, all formulae for the Monte Carlo simulation remain unchanged except for the value of σ_c and the same sample of random vectors $(x_i,\ i = 1,\ldots,n)$ can be used throughout the lifetime of the structure.

Notwithstanding the fact that crack growth is a complicated statistical phenomenon and is properly described by some sort of stochastic process /17 - 19/ it is felt that random crack growth can be modelled with sufficient accuracy by introducing an additional random variable. A theoretical justification for this procedure is given in /20/. If the constant C in eqn. (2.7) is random with probability density f(C), the time dependent failure probability is given by

$$Q_1 = \int_0^\infty f\,(C)\;Q_1(C)\;dC \tag{2.10}$$

with $Q_1(C)$ determined by eqn. (2.9). This implies that the sample for the Monte Carlo simulation now consists of the random vectors $x_i = (a_{oi}, (a/c)_{oi}, C_i, (\sigma_f)_i, (K_{Ic})_i)$. From eqn. (2.10) follows that a given crack grows with one and only one value of C.

2.2.2 Leak before Break Behavior

A two-dimensional crack can lead to either local or global failure of a component. Let σ_{2D} be the critical stress of a two-dimensional crack of given length c and given depth a; σ_{2D} also depends on material parameters such as K_{Ic} and σ_f. Let σ_{1D} be the critical stress of a through-wall crack of length c with the same material parameters. If the applied stress at the location of the two-dimensional crack exceeds σ_{2D}, the crack will become unstable and penetrate the wall which will lead to a one-dimensional crack of approximately the same length c (leak). In case of $\sigma \geq \sigma_{1D}$ this local instability will result in a global instability (break) and a complete failure of the component under consideration, whereas the one-dimensional crack will remain stable for $\sigma < \sigma_{1D}$.

For a crack with given geometry in a component with fixed material properties, the probabilities of obtaining leak, break or no failure depends on the stress distribution. We have:

$$P_{No\ failure} = P\ (\sigma < \sigma_{2D}) \tag{2.11}$$

$$P_{Leak} = \Theta\ (\sigma_{1D} - \sigma_{2D}) \cdot P\ (\sigma_{2D} \leq \sigma < \sigma_{1D}) \tag{2.12}$$

$$P_{Break} = P\ (\sigma \geq \max\ (\sigma_{1D}\ ,\ \sigma_{2D})) \tag{2.13}$$

where Θ is the step function.
Clearly global instability will always follow local instability if $\sigma_{2D} > \sigma_{1D}$.

Eqns. (2.11)-(2.13) have to be changed if the time history of a component is taken into account. The critical stresses σ_{2D} and σ_{1D} decrease with time due to cyclic crack growth. Let us assume that no leak has occurred for up to N_o load cycles, i.e. $P_{No\ failure} + P_{Break} = 1$. At $N = N_o$, we have $\sigma_{2D}(N_o) < \sigma_{1D}(N_o)$ and leakage can occur. If we now try to evaluate the various probabilities at $N_1 > N_o$, we have to compare the actual critical stresses $\sigma_{1D}(N_1)$, $\sigma_{2D}(N_1)$ with the values evaluated at the previous load cycle N_o and the critical stress $\sigma_{1D}(N_1, N_o)$ of the through-wall crack that has been formed at load cycle N_o with the length $c(N_o)$ and has now grown to the length $c(N_1)$. The following cases have to be distinguished:

1) $\sigma_{2D}\ (N_1) < \sigma_{2D}\ (N_0) \leq \sigma_{1D}\ (N_1)\ ,\ \sigma_{1D}\ (N_1,\ N_0) > \sigma_{2D}\ (N_0)$

The leak probability is given by the probability that the through-wall cracks formed at cycle N_o did not yet lead to a global failure and the probability that leakage occurs:

$$P_{Leak}(N_1) = P(\sigma_{2D}(N_0) \le \sigma < \sigma_{1D}(N_1, N_0)) + P(\sigma_{2D}(N_1) \le \sigma < \sigma_{2D}(N_0))$$

$$= P(\sigma_{2D}(N_1) \le \sigma < \sigma_{1D}(N_1, N_0)) \quad (2.14)$$

The probabilities of no failure and of breakage are given by:

$$P_{Break}(N_1) = P(\sigma \ge \sigma_{1D}(N_1, N_0)) \quad (2.15)$$

$$P_{No\ failure}(N_1) = P(\sigma < \sigma_{2D}(N_1)) \quad (2.16)$$

2) $\sigma_{2D}(N_1) < \sigma_{2D}(N_0) \le \sigma_{1D}(N_1)$, $\sigma_{1D}(N_1, N_0) \le \sigma_{2D}(N_0)$

In this case we obtain

$$P_{Leak}(N_1) = P(\sigma_{2D}(N_1) \le \sigma < \sigma_{2D}(N_0)) \quad (2.17)$$

$$P_{Break}(N_1) = P(\sigma \ge \sigma_{2D}(N_0)) \quad (2.18)$$

$$P_{No\ failure}(N_1) = P(\sigma < \sigma_{2D}(N_1)) \quad (2.19)$$

3) $\sigma_{2D}(N_1) < \sigma_{1D}(N_1) < \sigma_{2D}(N_0)$, $\sigma_{1D}(N_1, N_0) \le \sigma_{2D}(N_0)$

yields

$$P_{Leak}(N_1) = P(\sigma_{2D}(N_1) \le \sigma < \sigma_{1D}(N_1)) \quad (2.20)$$

$$P_{Break}(N_1) = P(\sigma \ge \sigma_{1D}(N_1)) \quad (2.21)$$

$$P_{No\ failure}(N_1) = P(\sigma < \sigma_{2D}(N_1)) \quad (2.22)$$

4) $\sigma_{1D}(N_1) \le \sigma_{2D}(N_1)$

reduces the leak probability to zero and we have:

$$P_{Break}(N_1) = P(\sigma \geq \sigma_{2D}(N_1)) \tag{2.23}$$

$$P_{No\ failure}(N_1) = P(\sigma < \sigma_{2D}(N_1) \tag{2.24}$$

Cases with $\sigma_{1D}(N_1, N_o) > \sigma_{1D}(N_1)$ need not be considered because a through-wall crack of length $c(N_o)$ grows faster than a two-dimensional crack of the same length.

In the next load cycle N_2 we have to keep track of both the leaks formed at N_o with the critical stresses $\sigma_{2D}(N_o)$ and $\sigma_{1D}(N_2, N_o)$ and the leaks formed at N_1 with the critical stresses $\sigma_{2D}(N_1)$ and $\sigma_{1D}(N_2, N_1)$. After k load cycles the contributions from previous leakages can be summarized as follows:

$$P_{Previous\ leaks}(N_k) = \sum_{i=0}^{k-1} \Theta(\sigma_{1D}(N_k, N_i) - \sigma_{2D}(N_i)) \cdot \cdot P(\sigma_{2D}(N_i) \leq \sigma < \min(\sigma_{2D}(N_{i-1}), \sigma_{1D}(N_k, N_i))) \tag{2.25}$$

with $\sigma_{2D}(N_{-1})$ equal to the upper bound of the stress distribution. New leaks occur with the probability:

$$P_{New\ leaks}(N_k) = \Theta(\sigma_{1D}(N_k) - \sigma_{2D}(N_k)) \cdot \cdot P(\sigma_{2D}(N_k) \leq \sigma < \min(\sigma_{2D}(N_{k-1}), \sigma_{1D}(N_k))) \tag{2.26}$$

from which the total leak probability is obtained:

$$P_{Leak}(N_k) = \sum_{i=0}^{k} \Theta(\sigma_{1D}(N_k, N_i) - \sigma_{2D}(N_i)) \cdot \cdot P(\sigma_{2D}(N_i) \leq \sigma < \min(\sigma_{2D}(N_{i-1}), \sigma_{1D}(N_k, N_i))) \tag{2.27}$$

with $\sigma_{1D}((N_k) = \sigma_{1D}(N_k, N_k))$.
Because of $\sigma_{2D}(N_k) < \sigma_{2D}(N_{k-1}) < \ldots < \sigma_{2D}(N_o)$ and $\sigma_{1D}(N_k, N_k) = \sigma_{1D}(N_k) > \sigma_{1D}(N_k, N_{k-1}) > \ldots > \sigma_{1D}(N_k, N_o)$ eqn. (2.27) can be simplified to

$$P_{Leak}(N_k) = P(\sigma_{2D}(N_k) \leq \sigma < \min(\sigma_{2D}(N_{j-1}), \sigma_{1D}(N_k, N_j))) \tag{2.28}$$

where j is the smallest index with $\sigma_{1D}(N_k, N_j) > \sigma_{2D}(N_j)$. Consequently, the probability for global instability is given by

$$P_{Break}(N_k) = P(\sigma \geq \min(\sigma_{2D}(N_{j-1}), \sigma_{1D}(N_k, N_j))) \tag{2.29}$$

If $\sigma_{1D}(N_k, N_j) < \sigma_{2D}(N_j)$ for all values of j, all leaks have become unstable and

$$P_{Leak} = 0$$

$$P_{Break} = P\ (\sigma \geq \sigma_{2D}\ (N_k)) \tag{2.30}$$

The failure probabilities calculated above apply only to cases with fixed initial crack geometry and fixed material properties, but can be easily generalized to random values of these quantities by multiplying with the corresponding probability densities:

$$Q_{Leak}\ (N_k) = \int_0^{\infty} f\ (K_{Ic}) \int_0^{\infty} f\ (\sigma_f) \int_0^{1} f\ ((a/c)_0) \int_0^{t} f\ (a_0)\ P_{Leak}\ (N_k)\ da_0\ d\ (a/c_0)\ d\sigma_f\ dK_{Ic} \tag{2.31}$$

and

$$Q_{Break}\ (N_k) = \int_0^{\infty} f\ (K_{Ic}) \int_0^{\infty} f\ (\sigma_f) \int_0^{1} f\ ((a/c)_0) \int_0^{t} f\ (a_0)\ P_{Break}\ (N_k)\ da_0\ d\ (a/c)_0\ d\sigma_f\ dK_{Ic} \tag{2.32}$$

In the Monte Carlo simulation the term $1 - F(\sigma = \sigma_c)$ in eqn. (2.4) is replaced by

$$P_{Leak}\ (N_k) = F\ (\sigma = \min\ (\sigma_{2D}\ (N_{j-1}),\ \sigma_{1D}\ (N_k,\ N_j))) - F\ (\sigma = \sigma_{2D}\ (N_k)) \tag{2.33}$$

for Q_{Leak} and by

$$P_{Break}\ (N_k) = 1 - F\ (\sigma = \min\ (\sigma_{2D}\ (N_{j-1}),\ \sigma_{1D}\ (N_k,\ N_j))) \tag{2.34}$$

for Q_{Break}. Consequently, the same set of random vectors can be used to determine Q_{Leak} and Q_{Break}. However, experience has shown that two different sets of importance sampling functions may be required in order to determine the failure integral for leak and break with satisfactory accuracy.

2.2.3 Periodic Inspection /16/

Components of high reliability such as airplanes or nuclear components have to undergo periodic non-destructive examinations in order to exclude dangerous fatigue damage caused by excessive fatigue crack growth. In probabilistic fracture mechanics the reliability of such non-destructive tests is assessed by a non-detection probability P_{ND}. Generally this probability depends strongly on the material and the geometry of the component inspected, but it is felt that a conservative approximation of the non-detection probability can be found which is applicable to a wide variety of components. If all cracks found during the inspection are removed and no additional cracks are introduced during the repair, the distribution of crack geometry after the inspection f_1 is related to the distribution prior to the inspection f_o by:

$$f_1\ (a,\ a/c) = f_0\ (a,\ a/c) \cdot P_{ND}\ (a,\ a/c) \qquad (2.35)$$

If the first inspection takes place before the components are put into service, the crack size distribution at start-up is modified to:

$$f\ (a,\ a/c) = C_N \cdot f_0\ (a,\ a/c) \cdot P_{ND}\ (a,\ a/c) \qquad (2.36)$$

with the normalization factor C_N:

$$C_N = \left(\int_0^t \int_0^1 f_0\ (a,\ a/c) \cdot P_{ND}\ (a,\ a/c)\ d\ (a/c)\ da \right)^{-1}$$

In eqn. (2.36) it is assumed that the distribution $f_o(a,a/c)$ of crack size and shape has been determined independently. If no information is available about this distribution prior to the inspection and the cracks found in the non-destructive examination are not removed we have:

$$f\ (a,\ a/c) = C_{ND}\ \ f_D\ (a,\ a/c) \cdot \frac{1}{1 - P_{ND}\ (a,\ a/c)} \qquad (2.37)$$

with

$$C_{ND} = \left(\int_0^t \int_0^1 f_D\ (a,\ a/c) \cdot \frac{1}{1 - P_{ND}\ (a,\ a/c)}\ d\ (a/c)\ da \right)^{-1}$$

where f_D denotes the distribution of cracks found in the component. f(a,a/c) as given in eqns. (2.36) or (2.37) has to be inserted in the formulae for the failure integral Q.

Let us now assume that the component undergoes cyclic loading and that an in-service inspection is performed after N_1 load cycles. Combining eqns. (2.36) and (2.8) gives:

$$f_1\,(a\,(N),\ a/c\,(N)) = f\,(a\,(N),\ a/c\,(N)) \cdot P_{ND}\,(a\,(N_1),\ a/c\,(N_1))$$

$$= f\,(a_0\,(a/c)_0) \cdot \left| \frac{\partial\,(a_0,\ (a/c)_0)}{\partial\,(a\,(N),\ a/c\,(N))} \right| \cdot P_{ND}\,(a\,(N_1).\ a/c\,(N_1)) \qquad (2.38)$$

and the failure integral $Q_1(N)$ eqn. (2.9) is changed into:

$$Q_1\,(N,\ N_1) = \int_0^\infty f\,(K_{Ic}) \int_0^\infty f\,(\sigma_f) \int_0^1 \int_0^t f\,(a_0,\ (a/c)_0) \cdot [1 - F\,(\sigma = \sigma_c\,(a\,(N),\ a/c\,(N)))]$$
$$\cdot\ P_{ND}\,(a\,(N_1),\ a/c\,(N_1))\ da_0\ d\,(a/c)_0\ d\sigma_f\ dK_{Ic} \qquad (2.39)$$

The failure probability at time $N > N_1$ of a component containing one and only one crack after one in-service inspection at N_1 is composed of two contributions:

$$Q_1^{(1)}\,(N,\ N_1) = [Q_1\,(N,\ N_1) - Q_1\,(N_1,\ N_1)] + Q_1\,(N_1) \qquad (2.40)$$

The first term accounts for the increase in the failure probability after the inspection whereas $Q_1(N_1)$ is the value of the failure integral just before the inspection took place.

If the next inspection is carried out after a total of N_2 load cycles, we have:

$$f_2\ (a\ (N),\ a/c\ (N)) = f_1\ (a\ (N),\ a/c\ (N))\ \ P_{ND}\ (a\ (N_2),\ a/c\ (N_2)) \tag{2.41}$$

$$= f\ (a_0,\ (a/c)_0) \cdot \left| \frac{\partial\ (a_0,\ (a/c)_0)}{\partial\ (a\ (N),\ a/c\ (N))} \right| \cdot P_{ND}\ (a\ (N_1),\ a/c\ (N_1))\ \ P_{ND}\ (a\ (N_2),\ a/c\ (N_2))$$

Eqn. (2.39) can be easily generalized to k inspections, wherefrom the final formula for the failure integral is obtained:

$$Q_1\ (N,\ N_1,\ .\ .\ .\ .\ ,\ N_k) = \int_0^\infty f\ (K_{Ic}) \int_0^\infty f\ (\sigma_f) \int_0^1 \int_0^t f\ (a_0,\ (a/c)_0) \cdot [1 - F\ (\sigma = \sigma_c\ (a\ (N_k),\ a/c\ (N_k)))]$$
$$\cdot \prod_{i=1}^{k} P_{ND}\ (a\ (N_i)\ ,\ a/c\ (N_i))\ da_0\ d\ (a,/c)_0\ d\sigma_f\ dK_{Ic} \tag{2.42}$$

The conditional failure probability after k inspections is given by:

$$Q_1^{(k)}\ (N,\ N_1,\ .\ .\ .,N_k) = Q_1\ (N,\ N_1,\ .\ .\ .,N_k) - Q_1\ (N_k,\ N_1,\ .\ .\ .\ .\ ,N_k) + Q_1^{(k-1)}\ (N,\ N_1,\ .\ .\ .,\ N_{k-1}) \tag{2.43}$$

2.2.4 Proof Test /21/

Pressure vessels or pipes have to undergo a pressure test before start-up to eliminate gross manufacturing errors such as very large cracks. Let the pressure test lead to a uniform stress σ_p throughout the component. If for a given combination of crack geometry and material parameters the critical stress is smaller than σ_p, failure will occur and the component will not be put into service. The failure probability eqn. (2.3) at the beginning of the component's life is modified to:

$$Q_1 = \int_0^\infty f\ (K_{Ic}) \int_0^\infty f\ (\sigma_f) \int_0^1 f\ (a/c) \int_0^t f\ (a)\ \ [\ 1 - F\ (\sigma = \sigma_c)] \cdot$$
$$\cdot\, \Theta\ (\sigma_c - \sigma_p)\ da\ d\ (a/c)\ d\sigma_f\ dK_{Ic} \tag{2.44}$$

This means for the Monte Carlo simulation that either each term in the sum of

Eq. (2.4) has to be multiplied by the step function $\Theta(\sigma_c(a_i, (a/c)_i) - \sigma_p)$ or that all terms with $\sigma_c < \sigma_p$ have to be removed from the sum and need not be considered in the course of the simulation.

2.2.5 Leak Detection

Pressurized components containing a liquid and failing by leakage are often connected to a leak detection system triggering a shutdown of the plant as soon as a critical leak rate L_c is exceeded. Generally, the leak rate L_R depends on the geometry of the crack causing the leak, the geometry of the pressurized component, and the pressure and the hydrodynamic properties of the liquid /10, 22/. On the assumption that /10/

$$L_R = l_1 (a, c) \sigma_{appl} + l_2 \tag{2.45}$$

where l_1 is a monotonically increasing function of the crack size and l_2 is a constant, a critical leak stress follows from $L_R = L_c$, namely.

$$\sigma_{Leak} = \frac{L_c - l_2}{l_1 (a,c)} \tag{2.46}$$

and a leak is detected for $\sigma_{appl} > \sigma_{Leak}$. A leak formed at a given time can either be detected immediately and repaired or continue to grow as a through-wall crack. Any reasonable leak detection system is designed such that a through-wall crack is detected before global instability occurs. In terms of critical stresses this implies that

$$\sigma_{1D} > \sigma_{Leak} \tag{2.47}$$

where σ_{1D} is the critical stress for global instability, holds for any crack geometry causing leakage.

If a given crack in a component with specific material properties can lead to a leak in the load cycle N_o, i.e. if $\sigma_{2D}(N_o) < \sigma_{1D}(N_o)$ (see Section 2.2.2), the leak probability P_{leak} Eq. (2.12) is split into two parts:

$$P_{Leak} (N_0) = P_{Leak, D} (N_0) + P_{Leak, ND} (N_0) \tag{2.48}$$

where

$$P_{Leak,\,D}\ (N_0) = P\ (\max\ (\sigma_{2D}\ (N_0),\ \sigma_{Leak}\ (N_0))\ \leq \sigma < \sigma_{1D}\ (N_0)) \tag{2.49}$$

is the probability of obtaining a detectable leak and

$$P_{Leak,\,ND}\ (N_0) = P\ (\sigma_{2D}\ (N_0) \leq \sigma < \sigma_{Leak}\ (N_0))\ \ \Theta\ (\sigma_{Leak}\ (N_0) - \sigma_{2D}\ (N_0)) \tag{2.50}$$

accounts for the leaks with leak rate below the critical leak rate. The probabilities of global instability, eqn. (2.13), and of no failure, eqn. (2.11) are, of course, not affected by the leak detection system.

At load cycle $N_1 > N_o$, the growth of the non-detected leaks formed up to now has to be considered in a way similar to the analysis of the leak-before-break behaviour. Because of the relation eqn. (2.47), leaks do not grow to final failure, but will be detected before becoming unstable, since σ_{Leak} decreases with increasing crack length and will eventually fall below the critical stress $\sigma_{2D}(N_o)$ determing leak formation.

Let $\sigma_{Leak}\ (N_i,\ N_j)$ denote the critical stress for detection at load cycle $N_i > N_j$ for a leak formed at load cycle N_j. Then it can be shown that at load cycle N_k the break probability is given by:

$$P_{Break}\ (N_k) = \sum_{i=0}^{k} P\ (\max\ (\sigma_{1D}\ (N_i),\ \sigma_{2D}\ (N_i)) \leq \sigma < \sigma_{2D}\ (N_{i-1}))$$
$$\cdot\ \Theta\ (\sigma_{2D}\ (N_{i-1}) - \sigma_{1D}\ (N_i)) \tag{2.51}$$

where $\sigma_{2D}(N_{-1})$ is equal to the upper bound of the stress distribution. The contribution to the leak probability from non-detected leaks follows from:

$$P_{Leak,\,ND}\ (N_k) = \sum_{i=0}^{k} P\ (\sigma_{2D}\ (N_i) \leq \sigma < \min\ (\sigma_{Leak}\ (N_k,\ N_i),\ \sigma_{2D}\ (N_{i-1}))) \cdot$$
$$\cdot\ \Theta\ (\sigma_{Leak}\ (N_k,\ N_i) - \sigma_{2D}\ (N_i)) \tag{2.52}$$

and detected leaks occur with the probability

$$P_{Leak,\,D} = \sum_{i=1}^{k} P\ (\max\ (\sigma_{Leak}\ (N_k,\ N_i),\ \sigma_{2D}\ (N_i)) \leq \sigma < \min\ (\sigma_{2D}\ (N_{i-1}),\ \sigma_{1D}\ (N_i))) \cdot$$
$$\cdot\ \Theta\ (\sigma_{1D}\ (N_i) - \sigma_{2D}\ (N_i)) \tag{2.53}$$

2.3 Differential Failure Probabilities /23/

In many cases of practical interest the available data base determining the input distributions in a PFM calculation is incomplete and does not allow to predict reliable values for the failure probabilities. However, PFM may still be useful if the attention is focused on trends and tendencies rather than on absolute numbers for the failure probabilities. Differential failure probabilities have been introduced for this purpose.
The PARIS code contains options for determining the differential failure probabilities for a, a/c, C, σ_f and K_{Ic}. For example, dQ_1/da is equal to:

$$\frac{dQ_1}{da} = f\,(a) \cdot \int_0^{\infty} f\,(K_{Ic}) \int_0^{\infty} f\,(\sigma_f) \int_0^{1} f\,(a/c) \quad [1 - F\,(\sigma = \sigma_c)]\ d\,(a/c)\ d\sigma_f\ dK_{Ic} \tag{2.54}$$

dQ_1/da is the probability of finding a crack of depth a in the component that leads to failure. Therefore, the differential failure probability for a can be considered as the distribution of hazardous cracks. A maximum in dQ_1/da at a certain crack depth a_o indicates that most of the failures observed are caused by cracks with depths of about a_o.

2.4 Determination of Importance Sampling Functions /24/

In many applications of probabilistic fracture mechanics very low values are obtained for the failure probabilities, so that great care has to be taken to control the numerical errors. Advanced Monte Carlo methods such as stratified sampling /10, 12/ and importance sampling /11, 12/ have been developed for variance reduction. In the PARIS code importance sampling is used, the basic ideas of which are described in section 1.2.

It is obvious from eqn. (1.14) that the gain in accuracy may vary considerably with the importance sampling function f_I. The PARIS code contains several features that can be used to determine optimum or at least satisfactory importance sampling functions. As a starting point we notice that the variance eqn. (1.14) is expected to be small if the ratio of the integrand in eqn. (1.7), f(a) h(a), and the importance sampling function $f_I(a)$ is approximately constant for all values of a. In a multi-dimensional problem such as eqn. (1.20) dQ_1/da (eqn. (2.53)) corresponds to the integrand, so that the simulation is expected to converge if the ratio of the differential failure probability and the importance sampling function is approximately constant. This can be achieved by fitting $f_I(a)$ to $(dQ_1/da)/Q_1$ using some standard curve fitting method.

These considerations lead to an iterative procedure applicable to any multi-dimensional failure probability such as eqn. (2.3). All but one random variables are kept constant at the beginning of the first iteration step and are assumed to be equal to their mean values or any other constant. Then $f_I(a)$ is determined by some curve fitting procedure such that it approximates

$$\frac{1}{Q_1} \cdot \frac{dQ_1}{da} = \frac{f\ (a) \cdot [1 - F\ (\sigma = \sigma_c)]}{\int_0^t f\ (a) \cdot [1 - F\ (\sigma = \sigma_c)]\ da} \tag{2.55}$$

as closely as possible. The importance sampling function is chosen to be any of the standard probability densities for which random number generators are available in the code. Q_1 is calculated from dQ_1/da by the trapezoid rule or any other numerical integration procedure.

The differential failure probability for the next variable, e.g. K_{Ic}, is obtained by a Monte Carlo simulation with the importance sampling function $f_I(a)$:

$$\frac{dQ_1}{dK_{Ic}} = f\ (K_{Ic}) \cdot \int_0^t \frac{f\ (a)}{f_I\ (a)} \cdot [1 - F\ (\sigma = \sigma_c)]\ dF_I\ (a) \tag{2.56}$$

The importance sampling function $f_I(K_{Ic})$, in turn, is determined by a fit to $(dQ_1/dK_{Ic})/Q_1$. Subsequent repetitions of this procedure lead to importance sampling densities for all input random variables. In some cases of practical interest it is necessary to start the iteration process from variables other than a in order to obtain a satisfactory variance reduction.

In the second step of the interation scheme, dQ/dx_i is calculated for each random variable x_i with the scatter of all other input quantities taken into account. Subsequent curve-fitting of a probability density function $f_I(x_i)$ to

Q^{-1} dQ_1/dx_i yields an improved estimate of near optimum importance sampling functions. The last step is repeated until two consecutive iterations lead to approximately the same importance sampling functions and the values of Q_1 determined by numerical integration of the dQ/dx_i vs x_i - curves remain constant.

3. Program Description

The PARIS code consists of a main program containing the Monte Carlo simulation and several subroutines, in which the fracture mechanical and statistical quantities required for the simulation are calculated.

3.1 The Main Program

The structure of the main program is shown in Fig. 3.1. First, the subroutine EINGAB is called, in which the user's input is read and stored in several COMMON blocks. A call of subroutine SEISMO generates the load cycles caused by earthquakes which are incorporated in the fatigue analysis performed in the course of the simulation. The Monte Carlo simulation is performed in several DO-loops. In the first loop, the coordinate WINKEL(IW) (IW = 1,..., NWIN) varies from WINKEL(1) to WINKEL(NWIN) so that components subjected to non-uniform stresses can be analyzed. For each value of WINKEL(IW) the applied stresses and cyclic loads are calculated by subroutine SPAWIN. Subroutine NORMIE yields the factor FNORM needed for proper normalization of all the distributions entering the simulation.

In the next step N random vectors (Z(I,1), Z(I,2), Z(I,3), Z(I,4), Z(I,5)), I = 1,..., N, are generated according to the user specified importance sampling distributions F_I. The first index IV = 1,..., 5 denoting the components of the random vector specifies the various input variables such as crack depth (IV = 1), aspect ratio (IV = 2), parameter of the crack growth law (IV = 3), flow stress (IV = 4) and fracture toughness (IV = 5). In the subsequent simulation loop the contribution of each of the N random vectors (Z (I, IV), IV = 1,...,5, I = 1,..., N) to the failure probability is calculated. First the ratio of the original densities and the importance sampling densities is determined:

$$\mathrm{FII} = \prod_{\mathrm{IV}=1}^{5} \frac{\mathrm{DVER\ (Z\ (IV,\ I),\ P1\ (IV),\ P2\ (IV),\ P3\ (IV),\ IVER\ (IV))}}{\mathrm{DVER\ (Z\ (IV,\ I),\ P1I\ \ (IV),\ P2I\ \ (IV),\ P3I\ \ (IV),\ IVERI\ (IV))}} \qquad (3.1)$$

where DVER is a subroutine containing various types of probability densities. P1(IV), P2(IV), P3(IV) and P1I(IV), P2I(IV), P3I(IV) denote the parameters of the original and the importance sampling distributions, respectively. IVER(IV), IVERI(IV) are indices specifying the type of the distribution under consideration.

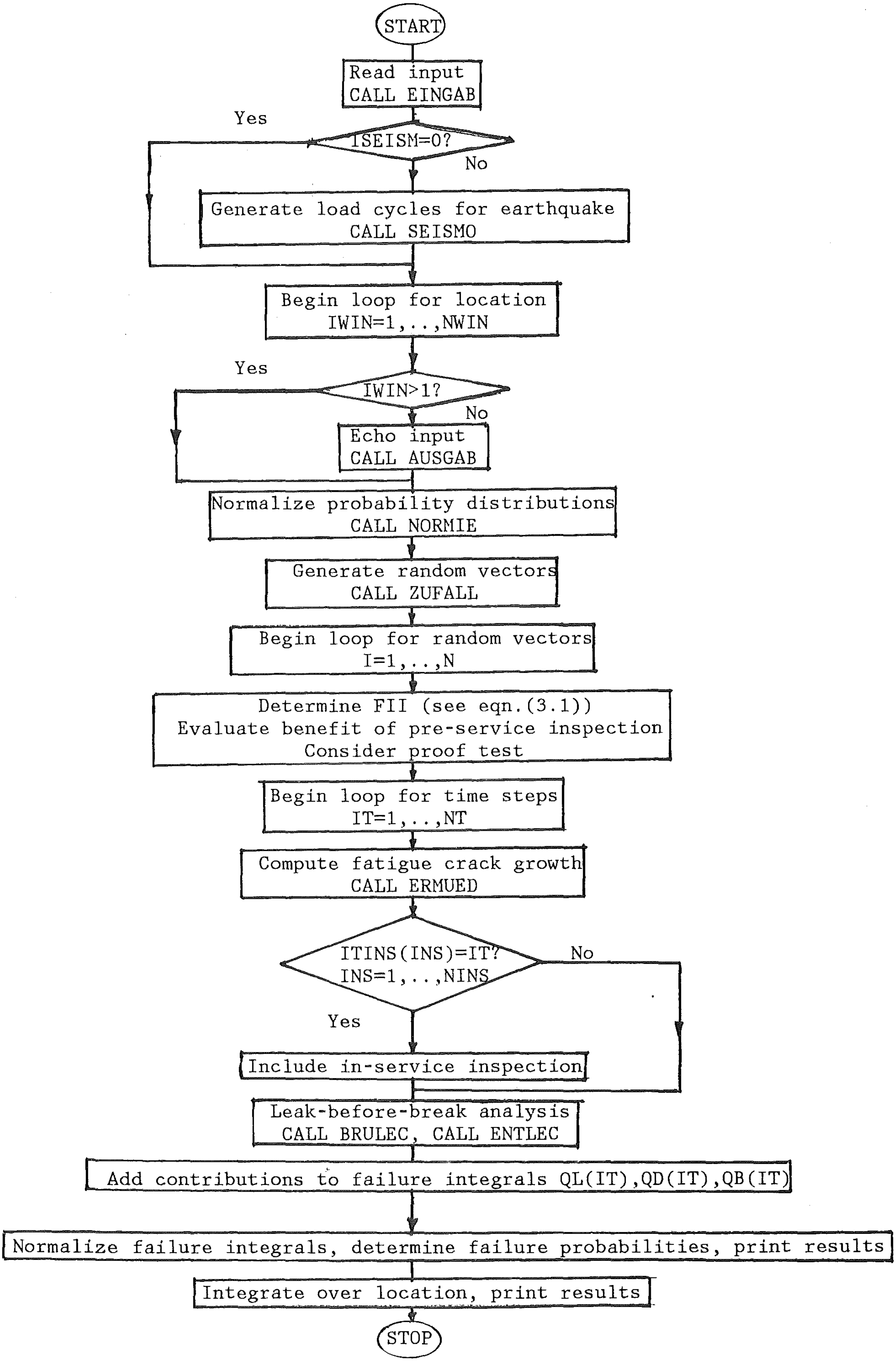

Figure 3.1 Flow chart of the main program of the PARIS code

A non-destructive inspection before start-up is taken into account by multiplying FII by the appropriate non-detection probability (see eqn. (2.36) or (2.37)). Subroutine VERSAG is called yielding the critical stress S2D at which the particular combination of crack geometry and material properties given by Z(IV, I), IV = 1,...,5, leads to failure. If a proof test with applied stress SIGP is performed, S2D $<$ SIGP implies that the corresponding random vector Z(., I) is removed from the subsequent calculations (see Section 2.2.4). Fatigue and leak-before-break behavior is analyzed in the following loop. For the sake of simplicity the total number of load cycles is divided into NT groups, each of which consisting of NDSIG different load amplitudes DSIG(IDSIG) occurring DFEQ(IDSIG) times (IDSIG = 1,..., NDSIG).

The crack growth caused by the load group IT (IT = 1, ..., NT) is determined in the subroutine ERMUED. As it was shown in Section 2.2.2., both the growth of the two-dimensional surface crack and of some one-dimensional through-wall cracks must be calculated once the leak probability is greater than zero.

The quantity ITINS(INS) indicates whether the component is inspected non-destructively after IT = ITINS(INS) load groups (INS = 1, ..., NINS; NINS is the total number of non-destructive inspections). This means that the joint probability density stored in FII (eqn. (3.1)) is multiplied by the non-detection probability PND(A,ADC), where A and ADC are the value of the crack depth and the depth to length ratio, respectively, after IT load groups (eqn. (2.42)) have been applied. Subroutines BRULEC(A, ADC, FISL, FISB) and ENTLEC(A, ADC, FISL, FISD, FISB) are called to perfom a probabilistic leak-before break analysis for the given crack of length A and depth-to-length ratio ADC (see sections 2.2.2 and 2.2.5); FISL = $P_{Leak,ND}$ denotes the probability for a leak which is not found, FISD = $P_{Leak,D}$ the probability for a leak which is detected by the leak detection system and FISB = P_{Break} the break probability. In the absence of a leak detection system, BRULEC determines the probability that the given crack causes local or global instability. A leak can either continue to grow stably during the component's lifetime or fail by global instability after some period of stable crack growth. ENTLEC takes into account the benefits of a leak detection system. A leak continues to grow until the leak rate is greater than a critical leak rate at which the through-wall crack is detected and repaired completely.

The next random vector Z(· , I + 1) is considered after NT time steps. Repeating this procedure for all random vectors and summing up the products FII*FISL, FII*FISD, FII*FISB etc. yields, after normalization, the failure integrals for non-detected leaks (QL(IT)), detected leaks (QD(IT)) and breaks (QB(IT)) at a given location of the component after IT groups of load cycles have occurred, together with the corresponding standard errors. If periodic inspections are performed after time steps ITINS(INS), these failure integrals are no longer equal to the corresponding failure probabilities but corrections have to be made according to eqns. (2.40), (2.43).

The total failure probability (eqn(1.1)) is equal to

$$AUST = 1 - EXP\ (\ -\ EM*(QL(IT)+QD(IT)+QB(IT))) \qquad (3.2)$$

where EM is the average number of cracks per component.

If the component considered is subject to varying stresses, the procedure described above has to be repeated for all NWIN locations. Numerical integration in the subroutine AUSWIN leads to the average failure integrals and the respective standard errors.

3.2 Fracture Mechanics Subroutines

These subroutines contain the relationships for calculating the growth of a given crack under cyclic loads and the critical stresses for leakage or break.

3.2.1 Stress Intensity Factors and Limit Loads

Various options for the stress intensity factor are available in subroutines TAKA(A,ADC,IK) and TAKB(A,ADC,IK). For one-dimensional cracks, only TAKA is called, whereas in two-dimensional cases, where both the depth A and the depth to length ratio ADC have to be taken into consideration, TAKA and TAKB yield the stress intensity factor at two specific ponts A and B along the crack front. If the applied stress is denoted by SIGMA, the stress intensity factors at A and B are

$$K_A = SIGMA*TAKA(A,ADC,IK) \text{ and } K_B = SIGMA*TAKB(A,ADC,IK), \qquad (3.3)$$

respectively.

The formulae for the various options for the stress intensity factor are contained in Appendix A.3. A specific crack and component geometry is selected by the index IK in the input. Table 3.1 gives a survey of the configurations assigned by IK.

Subroutine PG(ADC,IP) contains plastic limit loads for most of the geometries considered in TAKA and TAKB (see Table 3.2 and Appendix A.4). If SF denotes the flow stress of the material considered, the limit load is given by

$$\sigma_L = SF*PG(A,ADC,IP) \tag{3.4}$$

IP indicates which option is selected for the plastic limit load.

3.2.2 Critical Stress

The critical stresses S1D and S2D are determined in subroutine VERSAG(A,ADC, AKIC,SF,S1D,S2D), where S2D denotes the critical stress of a two-dimensional surface crack of the depth A and the depth-to-length ratio ADC and S1D the critical stress of a through-wall crack of the length A/ADC. AKIC is the fracture toughness and SF the flow stress. In the following IP1, IK1 refer to the crack model chosen for the one-dimensional through-wall crack whereas IP, IK denote the options selected for the two-dimensional crack. Both S1D and S2D are required, if a leak-before-break analysis is performed (see sections 2.2.2 and 2.2.5). Depending on the value of the index KRIT either a linear-elastic or a plastic or a elasto-plastic failure criterion is chosen. For KRIT = 1, we obtain from linear elastic fracture mechanics:

$$S1D = AKIC/TAKA(A(ADC,ADC,IK1)) \tag{3.5a}$$

$$S2D = AKIC/\max(TAKA(A,ADC,IK),TAKB(A,ADC,IK)), \tag{3.5b}$$

KRIT = 2 corresponds to the plastic limit load criterion yielding

$$S1D = SF*PG(A/ADC,ADC,IP1) \tag{3.6a}$$

$$S2D = SF*PG(A,ADC,IP) \tag{3.6b}$$

IK	CRACK MODEL	LOAD	REFERENCE
1	center cracked plate	tension	/38/
2	three-point-bend specimen	bending	/38/
3	longitudinal through-wall crack in pipe	internal pressure	/39/
4	circumferential through-wall crack in pipe	tension	/40/
5	circumferential through-wall crack in pipe	linear stress gradient	/41/
6	longitudinal through-wall crack in pipe	linear stress gradient	/42/
7	u s e r o p t i o n for through-wall crack		
8	semi-elliptical surface crack in plate	tension	/43/
9	semi-elliptical surface crack in plate	tension & bending	/43/
10	internal longitudinal semi-elliptical surface crack in pipe	internal pressure	/44/
11	internal longitudinal semi-elliptical surface crack in pipe	internal pressure	/30/
12	internal circumferential semi-elliptical surface crack in pipe	tension	/10/
13	external circumferential semi-elliptical surface crack in pipe	linear stress gradient	/41/,/43/
14	external longitudinal semi-elliptical surface crack in pipe	linear stress gradient	/41/,/43/
15	u s e r o p t i o n for two-dimensional crack		

Table 3.1 Survey of the options available for the stress intensity factor

IP	CRACK MODEL	LOAD	REFERENCE
1	center cracked plate	tension	/45/
2	three-point-bend specimen	bending	/45/
3	longitudinal through-wall crack in pipe	linear stress gradient	/46/
4	longitudinal through-wall crack in pipe	internal pressure	/47/
5	circumferential through-wall crack in pipe	linear stress gradient	/41/
6	circumferential through-wall crack in pipe	tension	/10/
7	longitudinal through-wall crack in pipe	linear stress gradient	/42/
8	u s e r o p t i o n for through-wall crack		
9	semi-elliptical surface crack in plate	tension	/45/
10	semi-elliptical surface crack in plate	tension	/48/
11	semi-elliptical surface crack in plate	tension	/25/
12	semi-elliptical surface crack in plate	tension & bending	/25/
13	external longitudinal semi-elliptical surface crack in pipe	internal pressure	/46/
14	internal circumferential semi-elliptical surface crack in pipe	tension	/10/
15	u s e r o p t i o n for two-dimensional crack		

Table 3.2 Survey of the options available for the plastic limit load

For KRIT = 3, the two-criteria approach of CEGB /25/ is used to describe elasto-plastic failure:

$$S1D,\ S2D = \frac{2}{\pi} * SIGL * ACOS\ (EXP(- \frac{\pi^2}{8} * \left(\frac{SIGK}{SIGL} \right)^2)) \tag{3.7}$$

where SIGK is the linear elastic critical stress given by eqn. (3.5a) for S1D and by eqn. (3.5b) for S2D, and SIGL the plastic limit load eqn. (3.6a) or (3.6b).

3.2.3 Crack Growth

Subroutine ERMUED(AA,CA,AE,CE) integrates the crack growth law eqn.(2.7). At a given time step IT, ERMUED determines the final depth AE and length CE of a crack with initial depth AA and length CA after NDSIG load cycles. There are two different options IFAT for the numerical integration of eqn. (2.7). IFAT = 1 calls DVERK, a subroutine contained in the IMSL library /26/ using a fifth order Runge-Kutta method. IFAT = 2 adds the increments Δa = YPRIME(1), Δc = YPRIME(2) (see below) caused by a load cycle of amplitude DSIG(IDSIG) to the actual crack depth and length. This method, albeit less accurate, is faster than the Runge-Kutta method and should preferably be chosen for load cycles with high frequencies DFEQ(IDSIG). As it is the case for the failure stress, the leak-before-break analysis requires that one-dimensional cracks are considered in addition to the two-dimensional crack. Therefore, the one-dimensional crack growth law for cracks of length CL is integrated in the second part of ERMUED.

The crack growth law integrated in ERMUED is stored in function FKN(ND,X,Y, YPRIME). Depending on the value of ND, a one- (ND = 1) or a two-dimensional (ND = 2) crack is considered. X denotes the number of load cycles, Y(1), Y(2) are the crack depth and length, and YPRIME(1), YPRIME(2) stand for the derivatives da/dN, dc/dN. FKN contains several different crack growth laws which can be selected by specifying the variable IERM. The following options are available:

IERM = 1

$$\frac{da}{dN} = CP * DK ** EN \qquad \text{for} \quad DK > DKTHR \tag{3.8}$$

IERM = 2

$$\frac{da}{dN} = \frac{CP * DK ** EN}{(1 - R) ** (EN * OM)} \quad \text{for} \quad \frac{DK}{(1 - R) ** OM} \geq DKTHR \tag{3.9}$$

IERM = 4

$$\frac{da}{dN} = \frac{CP * DK ** EN}{(1-R) * AKIC - DK} \quad \text{for } DK \geq DKTHR \tag{3.10}$$

EN, OM are material constants, CP = Z(IV = 3,I) also depends on the material but is assumed to be random, R is the ratio of minimum and maximum applied stress, AKIC is the fracture toughness, and DKTHR is the threshold value for fatigue crack growth. DK is the amplitude of the stress intensity factor and has to be evaluated at two different points if two-dimensional crack growth is considered.

IERM = 3 calls function RWASME(DK) containing a tri-linear form of crack growth law as given in the ASME code /30/:

$$da/dN = \begin{cases} CP1*DK**EN1 \text{ for } DKTHR1 \leq DK < DKTHR \\ CP*DK**EN \text{ for } DKTHR \leq DK < DKTHR3 \\ CP3*DK**EN3 \text{ for } DKTHR3 \leq DK \end{cases} \tag{3.11}$$

In some applications it may be necessary to specify time steps IT such that there are some load cycles occurring only DFEQ < 1 times per time step. A typical example are load cycles caused by major accidents. Subroutine FREQ(IT,NT,IKH) determines whether such a load cycle should be taken into account at a given time step IT (IKH = 1) or ignored (IKH = 0).

If an earthquake is included in the analysis (ISEISM = 1), additional load cycles caused by the earthquake have to be accounted for and NDSIG = NDSIG+1. Subroutine SEISMO(SERD,RATERD,FEQERD) determines whether an earthquake will actually occur at time step IT and what are the stress amplitude SERD, the stress ratio RATERD and the number of load cycles FEQERD to be used in the subsequent crack growth analysis. The earthquake currently modeled in the code is taken from /31/; any other model can easily be included by changing SEISMO.

3.2.4 Stress Gradients

Subroutine SPAWIN(X) enables the user to specify fatigue and applied loads varying with the location of the crack considered. The stress amplitude of each load cycle, DSIG(IDSIG), is a product of a dimensionless amplitude DSMAX(IDSIG) defined in the input and a stress factor SMEM depenent on the location of the crack. It is assumed that the stresses caused by fatigue loads can be described in terms of a fourth order polynominal:

$$\begin{aligned} \text{SIG1} &= \text{BI}(5)*\text{X}**4+\text{BI}(4)*\text{X}**3+\text{BI}(3)*\text{X}**2+\text{BI}(2)*\text{X}+\text{BI}(1) \\ \text{SIG2} &= \text{BA}(5)*\text{X}**4+\text{BA}(4)*\text{X}**3+\text{BA}(3)*\text{X}**2+\text{BA}(2)*\text{X}+\text{BA}(1) \end{aligned} \tag{3.12}$$

where SIG1 is the stress on the outer surface of the component, SIG2 is the stress on the inner surface, X is the location and BI(J), BA(J), J = 1,..,5, are coefficients specified in the input. SPAWIN assumes that a linear gradient exists between inner and outer surfaces which can be described as the superposition of a membrane stress

$$\text{SMEM} = (\text{SIG1} + \text{SIG2})/2. \tag{3.13}$$

and a bending stress (SIG1-SIG2)/2. This bending stress is taken into account in the stress intensity factor by introducing the quantity

$$\text{FAKERM} = (\text{SIG1} - \text{SIG2})/(\text{SIG1} + \text{SIG2}) \tag{3.14}$$

The method described above is also applied to the failure stress. The stresses at the outer and inner surface are denoted by SIGV1, SIGV2 with

$$\begin{aligned} \text{SIGV1} &= \text{BVI}(1)+\text{BVI}(2)*\text{X}+\text{BVI}(3)*\text{X}**2+\text{BVI}(4)*\text{X}**3+\text{BVI}(5)*\text{X}**4 \\ \text{SIGV2} &= \text{BVA}(1)+\text{BVA}(2)*\text{X}+\text{BVA}(3)*\text{X}**2+\text{BVA}(4)*\text{X}**3+\text{BVA}(5)*\text{X}**4 \end{aligned} \tag{3.15}$$

The membrane stress SIGV = (SIGV1+SIGV2)/2. defines the parameter P1(6) of the stress distribution in the Monte Carlo simulation. The other parameters of the stress distribution are assumed to be independent of the location. The bending component of the applied stress is accounted for by the factor

$$FAKVER = (SIGV1 - SIGV2)/(SIGV1 + SIGV2) \tag{3.16}$$

in the stress intensity factor and the limit load.

3.3 Statistical Subroutines

3.3.1 Distribution Functions

The probability distributions used in the Monte Carlo simulation are contained in FUNCTION DVINT(X,P1,P2,P3,IFLAG); FUNCTION DVER(X,P1,P2,P3,IFLAG) gives the corresponding probability densities. Depending on the value of the variable IFLAG, an exponential, a log-normal, normal, Weibull, gamma, uniform or extreme value distribution is selected. All these distributions depend on maximal three parameters P1, P2, P3 and may have an additional upper bound (OG) and lower bound (UG). The details can be found in Appendix A.1. FUNCTION DVINT is related to FUNCTION DVER by:

$$DVINT\ (Y, P1, P2, P3, IFLAG) = \int_{UG}^{Y} DVER\ (X, P1, P2, P3, IFLAG)\ dX \tag{3.17}$$

If one of the input variables is assumed to be a constant (IFLAG = 8), DVER and DVINT are equal to 1, so that eqn. (3.1) can be applied without any further changes.

In the course of the simulation, DVER is used both for the "original" probability densities and for the importance sampling functions. In the first case, the input quantities P1(IV), P2(IV), P3(IV), IVER(IV) replace P1, P2, P3, IFLAG in the probability density of the random variable IV, whereas P1I(IV), P2I(IV), P3I(IV), IVERI(IV) specify the corresponding importance sampling distribution. Both distributions have the same lower and upper bound denoted by UG(IV) and OG(IV), respectively. Generally, the distributions are not normalized for finite lower and upper bounds, and a normalization factor has to be calculated by subroutine NORMIE (see Section 3.3.4).

3.3.2 Random Number Generators

In the Monte Carlo simulation, various kinds of random numbers have to be generated depending on the importance sampling distribution F_I, which is done in subroutine ZUFALL(Z,N). The random numbers are stored in the array

Z(IV,I), where IV denotes the components of the random vector Z(, I) and I = 1,...,N. N is the total number of random numbers generated. The following random number generators of the IMSL-library /26/ are used: GGUBFS for uniform distributions, GGNQF for normal distributions and GGAMR for gamma distributions. All the other random number generators required can be derived from those with the help of some arithmetic transformations. The details can be found in Appendix A.2.

3.3.3 Non-Detection Probability

Non-destructive examinations of a component containing cracks may be performed at the beginning of its lifetime or during service. Eqns. (2.36), (2.37), 2.41) indicate the change in the crack geometry distribution for the case that the reliability of the non-destructive test is expressed in terms of a non-detection probability P_{ND}.

The input variable IAVER determines for an inspection before start-up whether the input crack geometry distribution is considered to represent the distribution of the cracks actually existing in the component (IAVER = 1) or the distribution of the cracks found during the pre-service inspection (IAVER = 2). The following non-detection probabilities are available in FUNCTION PND(A, ADC) in the PARIS code and can be selected by the input variable IPND:

IPND = 1: no inspection

IPND = 2 /32/ PND = PINS(3)+(1-PINS(3))*EXP(-PINS(1)*A) (3.18)

IPND = 3 /31/

$$\text{PND} = \begin{cases} 1 \text{ for A} < \text{PINS(2)} & (3.19) \\ \text{PINS(3)+(1-PINS(3))*EXP(-PINS(1)*(A-PINS(2))) for A} \geq \text{PINS(2)} & \end{cases}$$

IPND = 4 /10/ PND = PINS(3)+(1-PINS(3))*0.5*ERFC(PINS(4)+ln(AR/AF)) .

where AR = A*min(2*A/ADC, PINS(2))

(3.20)

AF = PINS(1)*PINS(2)

and ERFC is the complement of the error function.

IPND = 5 /33/

$$PND = PINS\ (3) + (1 - PINS\ (3)) * ERFC\ \left(\frac{ALOG\ (A/(DICK * PINS\ (1)))}{\sqrt{2} * PINS\ (2)}\right) \tag{3.21}$$

The parameters PINS(1),..., PINS(4) are input variables. In-service inspections take place when the input quantity ITINS(INS), INS=1, ..., NINS is equal to IT, i.e. after the ITth load group has been applied (see 3.1). NINS is the total number of in-service inspections.

3.3.4 Normalization

Probability theory requires all distributions in the Monte Carlo simulation to be normalized such that

$$\int_{UG}^{OG} f\ (x)\ dx = 1 \tag{3.22}$$

As the distributions in FUNCTION DVER are only normalized, if the upper and lower bounds coincide with the domain of the distribution, a normalization factor FNORM is determined in subroutine NORMIE(FNORM). If FN(IV) with

$$FN\ (IV) = \int_{UG(IV)}^{OG(IV)} DVER\ (X,\ P1\ (IV),\ P2\ (IV),\ P3\ (IV),\ IVER\ (IV))\ dX \tag{3.23}$$

is the normalization factor of the random variable IV, and FNI(IV) given by

$$FNI(IV) = \int_{UG(IV)}^{OG(IV)} DVER\ (X,\ P1I\ (IV),\ P2I\ (IV),\ P3I\ (IV),\ IVERI\ (IV)\ dX \tag{3.24}$$

the normalization factor of the corresponding importance sampling distribution, FNORM is equal to

$$FNORM = \prod_{IV=1}^{IZAHL-1} \frac{FNI(IV)}{FN\ (IV)} \cdot \frac{1}{FN\ (IZAHL)} \tag{3.25}$$

where IZAHL = 6 denotes the number of random variables taken into account in the simulation. The random variable IV = IZAHL corresponds to the stress distribution which enters the failure probability only in terms of its probability distribution (see Section 2.1). If the component considered is inspected non-destructively before start-up, the normalization factor for the crack geometry distribution is determined by

$$\mathrm{FN}\ (1) * \mathrm{FN}\ (2) = \int_{\mathrm{UG}(1)}^{\mathrm{OG}(1)} \int_{\mathrm{UG}(2)}^{\mathrm{UG}(2)} f\ (a)\ f\ (a/c)\ P_{ND}\ (a,\ a/c)\ d\ (a/c)\ da \tag{3.26a}$$

for IAVER = 1 and

$$\mathrm{FN}\ (1) * \mathrm{FN}\ (2) = \int_{\mathrm{UG}(1)}^{\mathrm{OG}(1)} \int_{\mathrm{UG}(2)}^{\mathrm{OG}(2)} \frac{f\ (a) \cdot f\ (a/c)}{1-\mathrm{PND}\ (a, a/c)}\ d\ (a/c) \tag{3.26b}$$

for IAVER = 2.

The integrals in eqn. (3.23 - 3.24) are calculated in subroutine DVINT (see section 3.3.1) whereas the IMSL subroutine DBLIN yields the double integrals eqn. (3.26).

3.3.5 Probabilistic Leak-Before-Break Analysis

Subroutine BRULEC(A, ADC, FISL, FISB) determines the leak and the break probabilities if no leak detection systems is available, i.e. if the input quantity QLENT is equal to zero. First the critical stress S2D = σ_{2D} of the present two-dimensional crack with depth A and depth-to-length ratio ADC and the corresponding critical stress S1D = σ_{1D} of a one-dimensional crack of length A/ADC are determined in subroutine VERSAG. The index ILE numbers the previous time steps N_i at which the leak probability was different from zero and for which the critical stress of the through-wall crack S1LECK (ILE) = σ_{1D} (IT, N_i) is still larger than the corresponding two-dimensional value S2LECK (ILE) = σ_{2D} (N_i). The leak and break probabilities, eqn. (2.25) and eqn. (2.26), are denoted by FISL and FISB, respectively.

Subroutine ENTLEC(A, ADC, FISL, FISD, FISB) is called if the effect of a leak detection system on the reliability of the component is taken into account. As in BRULEC, the critical stresses S1D, S2D corresponding to the actual crack configuration A, ADC are determined in the first place. Then the critical leak stress σ_{Leak}(IT) = S1LENT(IT) is determined as well as the change in time of the critical leak stresses σ_{Leak}(IT, ILE) = S1LENT(ILE) for leaks formed at a previous load cycle ILE. Eqns. (2.50) - (2.52) are then applied yielding the probabilities $P_{Leak,ND}$ = FISL, $P_{Leak,D}$ = FISD and P_{Break} = FISB.

3.4 Miscellaneous

For components subjected to varying stresses, QB(IT), QL(IT), QD(LT) etc. are the failure probabilities at time IT and a given location WINKEL(IW). All locations are assumed to be equally probable, and numerical integration in subroutine AUSWIN(WINT) using the trapezoid rule yields the average failure probability WINT.

The critical stress for leak detection is determined in subroutine SIGENT(C). Harris /10/ derived the following relation for a pipe in a PWR:

$$\text{QLENT} = \text{SIGENT*C**2/CLE2} - \text{CLE1} \qquad (3.27)$$

where C is the crack length, the input quantity QLENT = L_c is the critical leak rate (in liter/sec) and σ_{Leak} = SIGENT is the critical stress for leak detection. The constants CLE1, CLE2 depend on the details of the mechanical and fluid-dynamic properties and are specified in the input.

FUNCTIONs AKOPT(A,ADC), BKOPT(A,ADC) contain the formulae for the stress intensity factor if the option IK = 15 is chosen (see Appendix A.2), FUNCTION AK1OPT(A) yields the one-dimensional K-factor for IK = 7. FUNCTIONs PG1OPT(A) and PG2OPT(A,ADC) are called for IP = 8 and IP = 15, respectively.

Subroutine SPAVER (SMAX) substitutes a narrow normal distribution for the step function eqn. (2.5) with

$$\begin{aligned} \text{P1} &= \text{SMAX} \\ \text{P2} &= 0.001\text{*SMAX} \\ \text{UG} &= 0.95\text{*SMAX} \\ \text{OG} &= 1.05\text{*SMAX} \end{aligned} \qquad (3.28a)$$

for positive applied stress SMAX and

$$\begin{aligned} P1 &= SMAX \\ P2 &= -0.001*SMAX \\ UG &= 1.05*SMAX \\ OG &= 0.95*SMAX \end{aligned} \tag{3.28b}$$

for negative applied stress SMAX.

Numerical integrals in the PARIS code are calculated with the IMSL-sub-routines DCADRE for one-dimensional integrals and DBLIN for two-dimensional integrals. Both require the integrand to be contained in external functions. Therefore, FUNCTIONs FGAMMA(X) (probability density of the gamma distribution) and FAPND2(ADC,A) (crack geometry distribution including pre-service inspection) are included in the code. FUNCTIONs AADC(A), BADC(A) give integration limits for DBLIN.

3.5 Input Description

Subroutine EINGAB reads the input data and stores them in various COMMON blocks. Table 3.3 shows how the input is organized. Table 3.4 gives an overview of the meaning and the range of the input variables. All READ statements are FORMAT-free. The first card contains the total number N of Monte Carlo simulations performed at a specific time step NT. If the appropriate importance sampling functions have been selected N = 1000-10,000 should be sufficient. Next, the average number EM of cracks per component has to be specified. In the PARIS code it is assumed that the actual number of cracks is Poisson distributed and, consequently, that the total failure probability is given by eqn. (3.2). The input quantity PAC determines whether the depth-to-length ratio a/c (PAC = 0) or the aspect ratio c/a (PAC > 0) is considered as an independent variable.

Next, the distributions of the independent random variables and their parameters are specified together with the corresponding importance sampling distributions. For each variable IV, the type of the distribution function is selected by IVER (IV), and the parameters of the distribution are given by P1(IV), P2(IV), P3(IV). Appendix A.1 contains a summary of the distributions available. UG(IV) and OG(IV) define the lower and the upper bound, respectively. IVERI(IV) and P1I(IV), P2I(IV), P3I(IV) specify the type and the parameters of the importance sampling distribution. IV = 1 corresponds to

N							
EM	PAC						
P1(1)	P2(1)	P3(1)	UG(1)	OG(1)	IVER(1)		
P1I(1)	P2I(1)	P3I(1)	IVERI(1)				
P1(2)	P2(2)	P3(2)	UG(2)	OG(2)	IVER(2)		
P1I(2)	P2I(2)	P3I(2)	IVERI(2)				
P1(3)	P2(3)	P3(3)	UG(3)	OG(3)	IVER(3)		
P1I(3)	P2I(3)	P3I(3)	IVERI(3)				
P1(4)	P2(4)	P3(4)	UG(4)	OG(4)	IVER(4)		
P1I(4)	P2I(4)	P3I(4)	IVERI(4)				
P1(5)	P2(5)	P3(5)	UG(5)	OG(5)	IVER(5)		
P1I(5)	P2I(5)	P3I(5)	IVERI(5)				
P1(6)	P2(6)	P3(6)	UG(6)	OG(6)	IVER(6)		
KRIT	IK	IP	IK1	IP1			
BREIT	DICK	RADIUS	ENY	NWIN			
*	WINKEL(1)	WINKEL(NWIN)					
BVI(1)	BVI(2)	BVI(3)	BVI(4)	BVI(5)			
BVA(1)	BVA(2)	BVA(3)	BVA(4)	BVA(5)			
SIGP	QLENT	CLE1	CLE2				
PINS(1)	PINS(2)	PINS(3)	PINS(4)	IPND	IAVER		
NT	NDSIG						
**	THR1	THR2					
**	BI(1)	BI(2)	BI(3)	BI(4)	BI(5)		
**	BA(1)	BA(2)	BA(3)	BA(4)	BA(5)		
**	EN	OM	DKTHR	IERM	IFAT	ISEISM	
**	EN1	EN3	CP1	CP3	DKTHR1	DKTHR3	DKTHR4
**	DSMAX(1)	DFEQ(1)	RATIO(1)				
**	..	..	..				
**	DSMAX(NDSIG)		DFEQ(NDSIG)		RATIO(NDSIG)		
**	NINS						
***	ITINS(1)						
***	..						
***	ITINS(NINS)						

* optional for NWIN > 1
** optional for NDSIG > 0
*** optional for NINS > 0

Table 3.3 Organization of input data

Variable	Definition and reference
BA(1),..,BA(5)	coefficients of fatigue stress, eqn. (3.12)
BI(1),..,BI(5)	coefficients of fatigue stress, eqn. (3.12)
BREIT	width of component; for pipes see eqn. (3.29); large number for plates; BREIT=DICK for 1D cracks
BVA(1),..,BVA(5)	coefficients of failure stress, eqn. (3.15)
BVI(1),..,BVI(5)	coefficients of failure stress, eqn. (3.15)
CLE1,CLE2	parameters for leak detection, eqn. (3.27)
CP1,CP3	parameters of the crack growth law, eqn. (3.11)
DFEQ(1),..,DFEQ(NDSIG)	frequency of load cycles per time step, see section 3.5
DICK	wall thickness of component
DKTHR	threshold value for cyclic crack growth, eqns. (3.8)-(3.11)
DKTHR1,DKTHR3,DKTHR4	parameters of the crack growth law, eqn. (3.11)
DSMAX(1),..,DSMAX(NDSIG)	relative stress amplitudes of load cycles, see section 3.5 and 3.11
EM	average number of cracks per component eqn.(3.2)
EN	parameter of crack growth laws eqns.(3.8)-(3.11)
ENY	Poisson's ratio
EN1,EN3	parameter of crack growth law, eqn. (3.11)
IAVER	indicates whether the input crack size distribution is determined from inspection data (IAVER=2) or known beforehand (IAVER=1)
IERM	selects crack growth law see eqns. (3.8)-(3.11)
IFAT	indicates whether the Runge-Kutta (IFAT=1) or a simplified procedure (IFAT=2) is taken to integrate the crack growth laws
IK	selects the stress intensity factor see Table (3.1) and App. A.2
IK1	selects the stress intensity factor of the through-wall crack used in the leak-before-break analysis, arbitrary for one-dimensional problems see Table (3.1) and App. A.2
IP	selects the plastic limit load, arbitrary for elastic problems, see Table 3.2 and App.A.3
IPND	selects the non-detection probability, eqns. (3.18)-(3.21)
IP1	selects the plastic limit load of the through-wall crack used in the leak-before-break analysis, arbitrary for one-dimensional problems, see Table 3.2 and App.A.3
ISEISM	indicates if en earthquake is considered (ISEISM=1) or not (ISEISM=0)
ITINS(1),..,ITINS(NINS)	time steps after which a non-destructive inspection will take place
IVER(1)	distribution type for crack depth a (App.A.1)
IVER(2)	distribution type for a/c or c/a "

Table 3.4 Definition of input variables

Variable	Definition and reference
IVER(3)	distribution type for parameter CP in eqns.(3.8)--(3.11) (App.A.1)
IVER(4)	distribution type for flow stress (App.A.1)
IVER(5)	distribution type for fracture toughness "
IVER(6)	distribution type for stress "
IVERI(1)	type of importance sampling distribution for a (App. A.1)
IVERI(2)	type of importance sampling distribution for a/c or c/a (App. A.1)
IVERI(3)	type of importance sampling distribution for parameter CP in eqns. (3.8)-(3.11) (App. A.1)
IVERI(4)	type of importance sampling distribution for flow stress σ_f (App. A.1)
IVERI(5)	type of importance sampling distribution for fracture toughness K_{Ic} (App. A.1)
KRIT	selects failure criterion, see section (3.2.2)
N	number of random vectors generated
NDSIG	number of load cycles per time step
NINS	number of in-service inspections
NT	number of time steps
NWIN	number of locations at which the failure probabilities are computed, NWIN=1 for uniform stress
OG(1)	upper bound of crack size distribution
OG(2)	upper bound of a/c (c/a) distribution
OG(3)	upper bound of the distribution of parameter CP
OG(4)	upper bound of flow stress distribution
OG(5)	upper bound of fracture toughness distribution
OG(6)	upper bound of stress distribution
OM	parameter of crack growth law eqn. (3.9)
PAC	indicates whether the distribution of the depth-to-length ratio (PAC=0.) or of the aspect ratio c/a is specified in the input (PAC>0.)
PINS(1),..,PINS(4)	parameters of the non-detection probability eqns. (3.18)-(3.21)
P1(1),P2(1),P3(1)	parameters of the crack depth distribution, see App. A.1
P1(2),P2(2),P3(2)	parameters of the a/c (c/a) distribution, see App. A.1
P1(3),P2(3),P3(3)	parameters of the distribution of the parameter CP in the crack growth laws eqns.(3.8)-(3.11), see App. A.1
P1(4),P2(4),P3(4)	parameters of the flow stress distribution, see App. A.1
P1(5),P2(5),P3(5)	parameters of the fracture toughness distribution, see App. A.1
P1(6),P2(6),P3(6)	parameters of the stress distribution, see App. A.1

Table 3.4 Definition of input variables

Variable	Definition and reference
P1I(1),P2I(1),P3I(1)	parameters of the importance sampling distribution for the crack size, see App. A.1
P1I(2),P2I(2),P3I(2)	parameters of the importance sampling distribution for a/c (c/a), see App. A.1
P1I(3),P2I(3),P3I(3)	parameters of the importance sampling distribution for the parameter CP in the crack growth laws eqns.(3.8)-(3.11), see App.A.1
P1I(4),P2I(4),P3I(4)	parameters of the importance sampling distribution for the flow stress, see App. A.1
P1I(5),P2I(5),P3I(5)	parameters of the importance sampling distribution for the fracture toughness, see App. A.1
QLENT	critical leak rate, eqn.(3.26), no leak detection is considered for QLENT=0.
RADIUS	inner radius of components, large number for plates
RATIO(1),..,RATIO(NDSIG)	R-value for load cycles, see eqns. (3.9), (3.10)
SIGP	critical stress for proof test, no proof test is considered for SIGP=0.
THR1,THR2	threshold for vibrations,see section 3.5, eqns. (3.29), (3.30)
UG(1)	lower bound for crack depth distribution
UG(2)	lower bound for a/c (c/a) distribution
UG(3)	lower bound for distribution of parameter CP
UG(4)	lower bound for flow stress distribution
UG(5)	lower bound for fracture toughness distribution
UG(6)	lower bound for for stress distribution
WINKEL(1),..,WINKEL(NWIN)	locations at which the failure integrals are computed, see section (3.1)

Table 3.4 Definition of input variables

the distribution of crack depth a, IV = 2 to the distribution of the depth-to-length ratio a/c or the aspect ratio c/a depending on the value of PAC. IV = 3 determines the distribution of the parameter CP in the crack growth laws eqn.(3.8) - (3.11), IV = 4 the distribution of flow stress σ_f and IV = 5 the distribution of fracture toughness K_{Ic}. No importance sampling distribution has to be specified for IV = 6, the distribution of the applied stress σ, as this distribution enters all the formulae for the failure integral in its integrated form only (see e.g. eqn. (2.2) - (2.4)).

The index KRIT on the following card selects one of the failure criteria (eqn. (3.5a) - (3.7)). IK specifies the stress intensity factor and IP the limit load (eqn. (3.3), (3.4)). In case of two-dimensional cracks (IK $\geq$ 8 and IP $\geq$ 9) a stress intensity factor (IK1) and a limit load (IP1) of a corresponding one-dimensional through-wall crack are needed for the leak-before-break analysis. Both IK1 and IP1 can take any value if only one- dimensional problems are considered.

The crack and component geometries attributed to the various values of IK, IP, IK1, IP1 are summarized in Appendix A.2. BREIT defines the width, DICK the thickness and RADIUS the inner radius of the component under consideration. For plates, RADIUS is arbitrary, whereas the following relation must be fulfilled for pipes

$$\text{BREIT} = \pi \cdot \text{RADIUS} \qquad (3.29)$$

ENY is Poisson's ratio .

The index NWIN specifies the number of locations WINKEL(IW) (IW = 1,...,NWIN) where the failure integral will be evaluated. For NWIN = 1, the lower and upper bounds WINKEL(1) and WINKEL(NWIN) are additional input variables. BVI(1),...,BVI(5) and BVA(1),...,BVA(5) are the coefficients of the polynomials eqn. (3.15) describing the variation of the applied stress throughout the component.

The following READ statement contains the stress SIGP applied during a proof-test before start-up, the critical leak rate QLENT and the constants CLE1, CLE2 determining the critical leak detection stress if a leak detection system has been installed. No proof test or no leak detection correspond to

SIGP = 0 or QLENT = 0.

PINS(1),.., PINS(4) are parameters of the non-detection probabilities eqns.(3.18) - (3.21) characterizing the efficiency of a pre-service or an in-service non-destructive inspection. The index IPND specifies which of the functions P_{ND} is selected. IAVER defines whether the input crack size distribution is taken as a distribution of cracks in the component before the inspection (IAVER = 1) or as the distribution of cracks found during the pre-service inspection (IAVER = 2).

The input variable NT defines the number of time steps, and NDSIG the number of different load cycles considered in the fatigue analysis. For NDSIG = 0 the failure probability is only calculated at start-up (IT = NT = 1) and no fatigue analysis is performed. The following input quantities are only relevant in case of NDSIG = 0 and can be omitted otherwise.

THR1 and THR2 are scaling variables used to speed up the integration of the crack growth law in case of load cycles with very high frequencies such as vibrations (see below). BI(1),.., BI(5) and BA(1),..., BA(5) are the coefficients of the reference stress for the fatigue analysis. EN and OM are the parameters in the crack growth law eqns. (3.8) - (3.11) selected by the index IERM, DKTHR is the corresponding threshold value. IFAT defines whether the Runge-Kutta method (IFAT = 1) or a simple iteration scheme (IFAT = 2) is used for the integration of the crack growth law. ISEISM specifies whether an earthquake is supposed to contribute to fatigue crack growth (ISEISM = 1) or not (ISEISM = 0). If the ASME crack growth law is chosen (IERM = 3), additional parameters EN1, EN3, CP1, CP3, DKTHR1, DKTHR3 have to be known according to eqn. (3.11). The NDSIG load cycles used in the fatigue analysis are given by their relative amplitudes DSMAX(IDSIG), their frequencies DFEQ(IDSIG) and their stress ratios RATIO(IDSIG) (IDSIG = 1,.., NDSIG). The actual values DSIG(IDSIG) of the stress amplitudes at a specific location are determined by multiplying DSMAX(IDSIG) by the corresponding value of the reference stress SMEM (eqn. (3.13)).

If a specific load cycle with relative amplitude DSMAX(IDSIG) occurs THR1 < DFEQ(IDSIG) < THR2 times an equivalent load cycle with a lower frequency

$$\text{DFEQ(IDSIG)} = \text{DFEQ(IDSIG)} / \text{THR1} \tag{3.30}$$

and a higher amplitude

$$DSMAX\ (IDSIG) = DSMAX * THR1 ** (1./EN) \tag{3.31}$$

will be calculated. This means that the right hand side in the crack growth law remains unchanged by the scaling procedure and fewer load cycles with higher amplitudes are equivalent to the original ones if there is no excessive crack growth during one cycle. In order to obtain the correct behaviour at the threshold of stable crack growth in terms of the transformed load cycles, the threshold DKTHR has to be changed accordingly:

$$DKTHR\ (IDSIG) = DKTHR * THR\ 1 ** (1./EN) \tag{3.32}$$

For DFEQ(IDSIG) > THR2 the scaling parameter THR1 is replaced by THR2.

3.6 Output Description

Subroutine AUSGAB prints all the input parameters together with some information about the options selected by the user. A typical print-out is shown in Table 3.5.

The results of the simulation are printed at the evaluation times NZEIT = IT - 1, IT = 1,..., NT where NT is the number of time steps. For non-uniform stresses (NWIN = 1) the averaged probabilities (eqn. (2.6)) are printed in addition to the values at each location WINKEL(IW) (IW = 1,..., NWIN). The break probabilities are listed as well as the leak probabilities which are divided into two parts, one accounting for the leak detected and repaired and the other for the leaks not found by the leak detection system. If no leak detection is considered, the first part of the leak probability vanishes.

As the simulation of the entire life of a component may be time consuming and the user may want to interrupt the programme at some intermediate time step, a special version of PARIS code is provided which after NT of a total of NTEND time steps stores the results in a file such that the program can be re-started.

```
**********************************************
************   P A R I S - C O D E   ************
**********************************************
PROBABILISTIC  ANALYSIS  OF  CRACKED  COMPONENTS
**********************************************


* NUMBER OF MONTE CARLO SIMULATIONS       1000
* AVERAGE NUMBER OF CRACKS PER COMPONENT    10.0000

* LOADING
    1. FATIGUE
    2. WITHOUT EARTHQUAKE
    3. WITHOUT VIBRATIONS
    4. STRESSES INDEPENDENT OF CRACK LOCATION

* FATIGUE CRACK GROWTH   SIMPLIFIED METHOD
    CRACK GROWTH LAW    ( W A L K E R )
     EXPONENT N  4.120      EXPONENT M 0.5000      DK(THRESHOLD)  240.0
     FATIGUE:    NUMBER OF TIME STEPS    5
     1 STRESS AMPLITUDE  60.1000     R 0.0           FREQUENCY  25.0000
     2 STRESS AMPLITUDE  42.0700     R 0.300000      FREQUENCY  200.000
     3 STRESS AMPLITUDE  6.01000     R 0.895000      FREQUENCY  250.000

* FAILURE CRITERION
     PLASTIC LIMIT LOAD

* COMPONENT -  LOADING  -  K-FACTOR
    WIDTH   860.0    THICKNESS  11.00    INNER RADIUS  273.9    NU 0.3000

   K-FACTOR FOR TWO-DIMENSIONAL CRACKS
    PIPE TENSION & BENDING     CIRCUMFERENTIAL CRACK  (ERDOGAN)

   K-FACTOR FOR ONE-DIMENSIONAL CRACKS
    PIPE TENSION & BENDING     CIRCUMFERENTIAL CRACK  (ERDOGAN)

   PLASTIC LIMIT LOAD FOR TWO-DIMENSIONAL CRACKS
    PLATE  TENSION & BENDING      (CEGB/R6)

   PLASTIC LIMIT LOAD FOR ONE-DIMENSIONAL CRACKS
    PIPE  TENSION & BENDING     CIRCUMFERENTIAL CRACK  (ERDOGAN)

* INSPECTION  AND  PROOF  TEST
    1. WITHOUT INSPECTION BEFORE START UP
    2. WITHOUT PROOF-TEST
    3. WITHOUT IN SERVICE INSPECTIONS
    4. WITHOUT LEAK DETECTION
```

Table 3.5 Print-out of the PARIS code

```
* DISTRIBUTED QUANTITIES

 CRACK DEPTH DISTRIBUTION
    PARAMETER P1=       1.00000       P2=   0.0           P3=   0.0
    LOWER BOUND =     0.100000D-04   UPPER BOUND =     11.0000
    NORMALIZATION=     1.00000
    EXPONENTIAL -   DISTRIBUTION
    IMPORTANCE-SAMPLING-DISTRIBUTION
    PARAMETER P1I=     9.04110       P2I=   0.957200    P3I=   0.0
    NORMIERUNG:    0.979646
    NORMAL -        DISTRIBUTION

 A/C- DISTRIBUTION
    PARAMETER P1=     0.520000       P2=   0.180000       P3=   0.0
    LOWER BOUND =     0.100000D-02   UPPER BOUND =     1.00000
    NORMALIZATION=    0.994174
    NORMAL -        DISTRIBUTION
    IMPORTANCE-SAMPLING-DISTRIBUTION
    PARAMETER P1I=    0.391000       P2I=   0.186000    P3I=   0.0
    NORMIERUNG:    0.981463
    NORMAL -        DISTRIBUTION

  DISTRIBUTION OF PARAMETER C
    PARAMETER P1=     0.538000D-15   P2=   0.780000       P3=   0.0
    LOWER BOUND =     0.0            UPPER BOUND =   0.100000D-06
    NORMALIZATION=     1.00000
    LOGNORMAL -     DISTRIBUTION
    IMPORTANCE-SAMPLING-DISTRIBUTION
    PARAMETER P1I=    0.520000D-15   P2I=   0.761600    P3I=   0.0
    NORMIERUNG:     1.00000
    LOGNORMAL -     DISTRIBUTION

 FLOW STRESS DISTRIBUTION
    PARAMETER P1=     258.900        P2=    18.9000       P3=   0.0
    LOWER BOUND =     5.00000        UPPER BOUND =     500.000
    NORMALIZATION=    1.00000
    NORMAL -        DISTRIBUTION
    IMPORTANCE-SAMPLING-DISTRIBUTION
    PARAMETER P1I=    253.600        P2I=    18.9980    P3I=   0.0
    NORMIERUNG:     1.00000
    NORMAL -        DISTRIBUTION

 KIC- DISTRIBUTION
    PARAMETER P1=     6500.00        P2=   0.0            P3=   0.0
    LOWER BOUND =     100.000        UPPER BOUND =     10000.0
    NORMALIZATION=    1.00000
    CONSTANT -      DISTRIBUTION
    IMPORTANCE-SAMPLING-DISTRIBUTION
    PARAMETER P1I=    6500.00        P2I=   0.0         P3I=   0.0
    NORMIERUNG:     1.00000
    CONSTANT -      DISTRIBUTION

 STRESS DISTRIBUTION
    PARAMETER P1=     60.1000        P2=   0.601000D-02  P3=   0.0
    LOWER BOUND =     0.0            UPPER BOUND =     60.1601
    NORMALIZATION=    1.00000
    NORMAL -        DISTRIBUTION

* * * NORMALIZATION     0.967121
```

T	Q-BREAK	SIGMA-BREAK	Q-LEAK(ND)	SIGMA-LEAK(ND)	Q-LEAK(D)	SIGMA-LEAK(D)	Q-TOTAL
0	0.315875D-06	0.222184D-06	0.209339D-03	0.843881D-05	0.0	0.0	0.209435D-02
1	0.545693D-06	0.256315D-06	0.219808D-03	0.134637D-04	0.0	0.0	0.220111D-02
2	0.163539D-05	0.109368D-05	0.220022D-03	0.134813D-04	0.0	0.0	0.221412D-02
3	0.177919D-05	0.110288D-05	0.219878D-03	0.134829D-04	0.0	0.0	0.221412D-02
4	0.182163D-05	0.110363D-05	0.220471D-03	0.134881D-04	0.0	0.0	0.222046D-02

Table 3.5: Print-out of the PARIS code

3.7 Differential Failure Probabilities

As it has been explained in Section 2.4, near optimum importance sampling distributions can be determined by an iterative procedure using differential failure probabilities. A special version (DIWA) of the PARIS code was developed with the purpose of calculating differential failure probabilities. In addition to the input necessary for the standard version of the code the user has to specify the variable IKON = 1,..., 5 with respect to which the failure probability is to be differentiated together with its lower (UKON) and upper bounds (OKON) and the number NSTEP of steps. DIWA then calculates dQ/dX(IKON) at points UKON < X (IKON) < OKON (IKON = 1,..., NSTEP). The total failure probability Q is estimated using the trapezoid rule. A curve fit of any of the standard distribution densities contained in subroutine DVER to $Q^{-1} \cdot$ dQ/dX(IKON) determines the importance sampling density for the variable IKON.

Experience has shown /14, 24, 34/ that 10-20 points X(IKON) are necessary for a curve fit of sufficient accuracy. In all examples considered up to now a maximum of NT = 2 time steps has been sufficient to define the importance sampling distribution for the entire design life of a specific component including up to NT = 40 time steps. Excessive crack growth, however, may lead to substantial changes in the differential failure probabilities in the component's lifetime and, consequently, to the necessity of using different importance sampling distributions for different time steps. In the examples studied up to now /14, 24, 34/, two or three iteration steps for each variable have led to stable values for the parameters of the importance sampling distributions.

4. Examples

In this section a PFM analysis is performed for a pipe elbow containing surface cracks in a circumferential weld with the purpose of illustrating some of the characteristic features of the PARIS code. The physical basis of the example is explained in /24/. The crack depth a, the depth-to-length ratio a/c, the flow stress σ_f and the parameter C of the crack growth law are assumed to be independent random variables. Due to cyclic service loads, the surface cracks grow stably until leakage or breakage occurs. Plastic collapse determines the critical stress σ_{1D}, σ_{2D} for local and global instabilities. Further details of the model are summarized in Table 4.1.

4.1 Determination of the Importance Sampling Distributions

As it has been explained in Section 2.4, an iteration scheme based on the differential failure probabilities can be used to determine suitable importance sampling distributions. With this method, the parameters of a specific importance sampling distribution can be calculated easily, but there is no way to determine the type of this distribution other than by guided guessing. A good starting point is to try the same type of probability density for $f_I(x)$ as f(x), the original probability density determining the statistical properties of the random variable x, because the differential failure probability is given by

$$\frac{dQ}{dx} = f(x) \cdot Q\ (x) \tag{4.1}$$

where Q(x) is the value of the failure integral evaluated at constant x. Once a suitable probability density is found, the iteration scheme normally converges after 2-3 steps.

Table 4.2 summarizes the results of the iteration scheme applied to the leak probability of the example. The only variable for which the importance sampling distribution differs from the type of the input distribution is the crack depth a. Fig. 4.1 illustrates that the exponential distribution is not a suitable choice for the corresponding importance sampling distribution, but that the normal distribution fits nicely. With 5000 simulation runs, the failure integral for leak at start-up, eqn. (2.31), turns out to be

Variable	Input quantity
Number of simulation runs	N=1000
Average number of cracks per component	EM=10.
Distribution of crack depth a	exponential, P1(1)=1., P3(1)=0., UG(1)=1.E-5, OG(1)=11.
Importance sampling distribution for a	
leak probability	normal, P1I(1)=9.041, P2I(1)=.957
break probability	Weibull, P1I(1)=4.41, P2I(2)=2.2, P3I(1)=0.
Distribution of depth-to-length ratio a/c	normal, P1(2)=.52, P2(2)=.18, UG(2)=1.E-3, OG(2)=1.
Importance sampling distribution for a/c	
leak probability	normal, P1I(2)=.391, P2I(2)=.186
break probability	lognormal, P1I(2)=.00514, P2I(2)=.825, P3I(2)=0.
Distribution of parameter CP	lognormal, P1(3)=5.38E-16, P2(3)=.78, P3(3)=0.,UG(3)=0., OG(3)=1.E-7
Importance sampling distribution for CP	
leak probability	lognormal, P1I(3)=5.2E-16, P2I(3)=.762,P3I(3)=0.
break probability	lognormal, P1I(3)=6.71E-16, P2I(3)=.872, P3I(3)=0.
Distribution of flow stress σ_f	normal, P1(4)=258.9, P2(4)=18.9 UG(4)=5., OG(4)=500.
Importance sampling distribution for σ_f	
leak probability	normal, P1I(4)=253.6, P2I(4)=19.
break probability	normal, P1I(4)=259.2, P2I(4)=19.2
Distribution of fracture toughness K_{Ic}	const., parameters arbitrary
Importance sampling distribution for K_{Ic}	
leak probability	const., parameters arbitrary
break probability	const., parameters arbitrary
Distribution of stress σ	constant, P1(5)=60., UG(5)=0., OG(5)=60.
Failure criterion	KRIT=2
Stress intensity factor	IK=13, pipe with external circumferential crack, linear stress gradient
Plastic limit load	IP=12, semi-elliptical surface crack in plate, tension & bending
Stress intensity factor of 1D crack	IK1=5, pipe with through-wall circumferential crack, linear stress gradient
Plastic limit load of 1D crack	IP1=5, pipe with through-wall circumferential crack, linear stress gradient

Table 4.1 Input for the example

Variable	Input quantity
Half circumference	BREIT=860.
Wall thickness	DICK=11.
Inner radius	RADIUS=273.9
Poisson's ratio	ENY=.3
Number of locations	NWIN=1
Coefficients of applied stress	BI(1)=65.6, BI(2)=..=BI(5)=0.
	BA(1)=54.4, BA(2)=..=BA(5)=0.
Proof-test	SIGP=0.
Leak detection	
no leak detection	QLENT=0., CLE1=1., CLE2=1.
with leak detection	QLENT=500., CLE1=0., CLE2=60.
Inspection	
no pre-service inspection	IPND=1,IAVER=1,PINS(1)=..=PINS(4)=0.
no in-service inspection	NINS=0
Number of time steps	NT=5, 1 time step = 1 year
Number of load cycles	NDSIG=3
Relative amplitudes of load cycles	DSMAX(1)=1.,DSMAX(2)=.7,DSMAX(3)=.1
Frequencies of load cycles	DFEQ(1)=25.,DFEQ(2)=200.,DFEQ(3)=250.
Ratios R of load cycles	RATIO(1)=0.,RATIO(2)=.3,RATIO(3)=.895
Threshold for vibrations	THR1=1000., THR2=1000.
Coefficients of fatigue stress	BVI(1)=65.6,BVI(2)=..=BVI(5)=0.
	BVA(1)=54.4,BVA(2)=..=BVA(5)=0.
Parameters of crack growth law	EN=4.12,OM=.5,DKTHR=240.,IERM=2
Integration of crack growth law	simple procedure,IFAT=2
Earthquake	none, ISEISM=0

Table 4.1 Input for the example

diff. failure prob. dQ/dx_j	constant variables	importance sampling probability distributions $F_I(a)$	$F_I(a/c)$	$F_I(\sigma_f)$	$F_I(C)$	failure integral Q_1
$x_j=a$	$a/c,\sigma_f,C$	normal, P1=9.23,P2=.81	---	---	---	1.6E-4
$x_j=a/c$	σ_f,C	normal, P1=9.23,P2=.81	normal, P1=.4,P2=.18	---	---	1.7E-4
$x_j=\sigma_f$	C	normal, P1=9.23,P2=.81	normal, P1=.4,P2=.18	normal, P1=253.,P2=19.	---	2.0E-4
----------	----------	---------end of first iteration------------				
$x_j=a$	C	normal, P1=9.04,P2=.97	normal, P1=.4,P2=.18	normal, P1=253.,P2=19.	---	1.9E-4
$x_j=a/c$	C	normal, P1=9.04,P2=.97	normal, P1=.39,P2=.186	normal, P1=253.,P2=19.	---	1.9E-4
$x_j=\sigma_f$	C	normal, P1=9.04,P2=.97	normal, P1=.39,P2=.186	normal, P1=254.,P2=19.	---	2.0E-4
----------	----------	---------end of second iteration-----------				
$x_j=a$	C	normal, P1=9.04,P2=.96	normal, P1=.39,p2=.186	normal, P1=254.,P2=19.	---	1.9E-4
$x_j=a/c$	C	normal, P1=9.04,P2=.96	normal, P1=.39,P2=.186	normal, P1=254.,P2=19.	---	1.9E-4
$x_j=\sigma_f$	C	normal, P1=9.04,P2=.96	normal, P1=.39,P2=.186	normal, P1=254.,P2=19.	---	2.1E-4
$x_j=C$ (*)	---	normal, P1=9.04,P2=.96	normal, P1=.39,P2=.186	normal, P1=254.,P2=19.	lognormal, P1=5.2E-16, P2=.76,P3=0.	1.7E-4
----------	----------	---------end of third iteration------------				

(*) evaluated at IT=2

Table 4.2 Determination of the importance sampling functions for the leak probabilities of the example

$$Q_{Leak}(0) = (1.94 \pm 0.03) \cdot 10^{-4} \tag{4.2}$$

An alternative approach to find suitable importance sampling distributions based on the first-order-second-moment method /35/ is described in /11,36/. Using this procedure we obtain with 5000 simulation runs

$$Q_{Leak}(0) = (1.99 \pm 0.04) \cdot 10^{-4} \tag{4.3}$$

which agrees very well with eqn. (4.2). In /14/ it was shown that the leak probability remains approximately constant throughout the component's lifetime. Therefore the same importance sampling distributions can be used for all time steps.

The break probability Q_{Break}, eqn. (2.32), and the corresponding differential failure probabilities, on the other hand, change rapidly during the first few load cycles so that a curve fit to dQ_{Break}/da or $dQ_{Break}/d(a/c)$ at start-up does not yield importance sampling distributions applicable to later time steps. Fig. 4.2 shows $f_I(a/c)$ and $Q_{Break}^{-1}\ dQ_{Break}/d(a/c)$ at start-up (IT = 1) and at IT = 2. Clearly $f_I(a/c)$ for IT > 1 cannot be based on the corresponding differential failure probability at start-up.

Fig. 4.3 reflects the influence of different sets of importance sampling functions on the simulation results. One set was determined using a Weibull distribution for $f_I(a)$, whereas the other was obtained with a lognormal distribution for $f_I(a)$. As the intervals spanned by the standard errors overlap, it can be inferred that there is no statistically significant deviation between the different sampling procedures.

4.2 Leak-Before-Break Analysis

An overview of the principles of the leak-before-break analysis described in Sections 2.2.2, 2.2.5 is given in Figs. 4.4 and 4.5. If the leak and break probabilities in eqns. (2.28), (2.29) and (2.50) - (2.52) were calculated by direct simulation, the flow charts Figs. 4.4 and 4.5 would illustrate the structure of the simulation program. Of course, the simulation procedure in the PARIS code is more involved so that these diagrams do not represent any part of the code, but only summarize which phenomena are accounted for in the leak-before-break analysis.

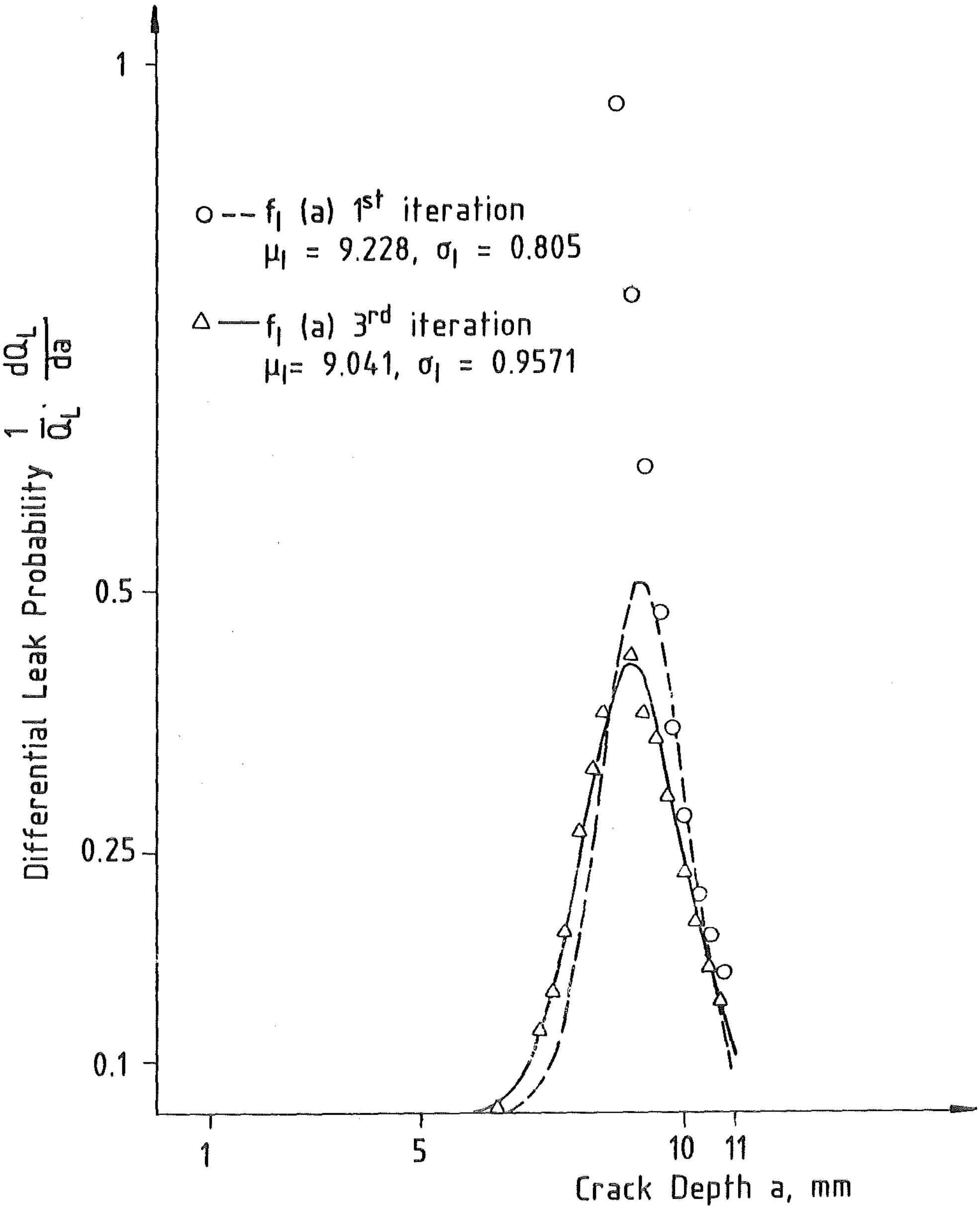

Figure 4.1 Determination of the importance sampling probability density $f_I(a)$ for the leak probability

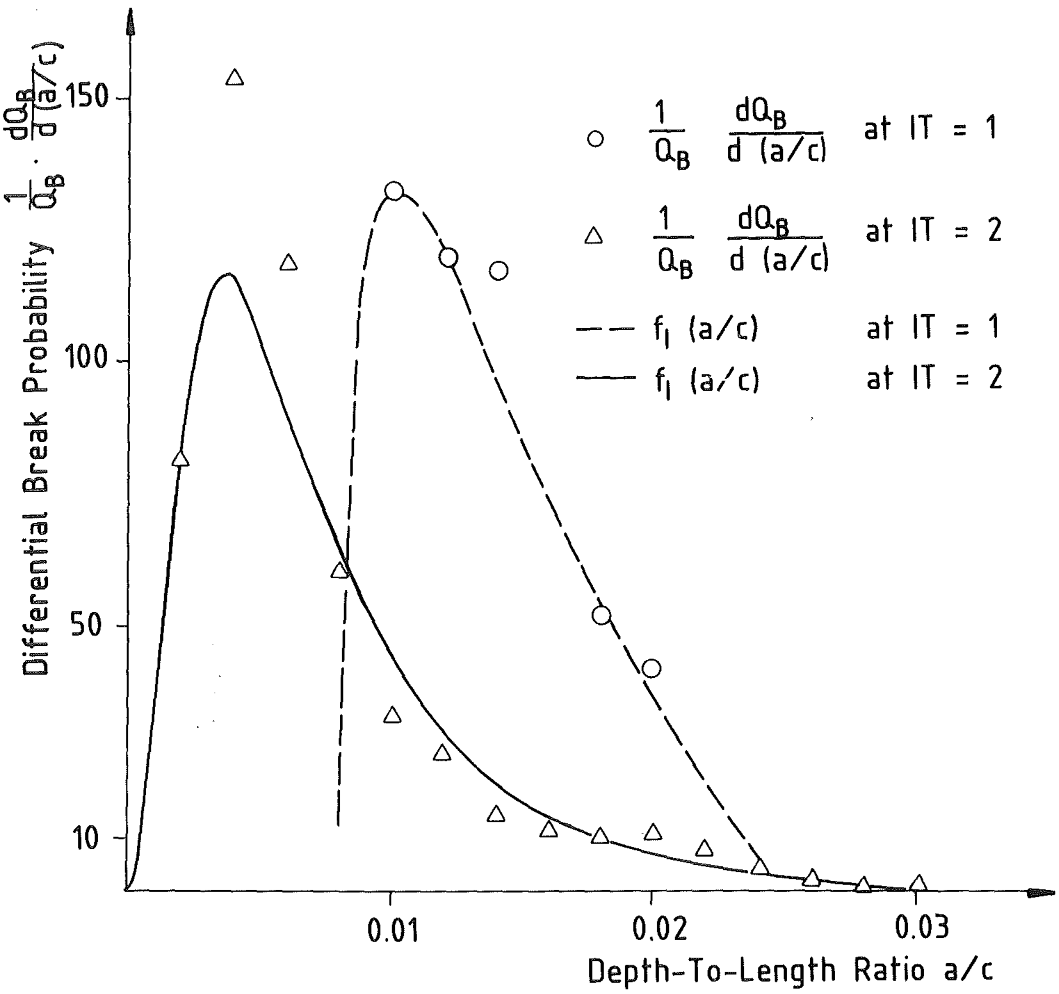

Figure 4.2 Determination of the importance probability density $f_I(a/c)$ for the break probability; time step IT = 1 corresponds to start-up

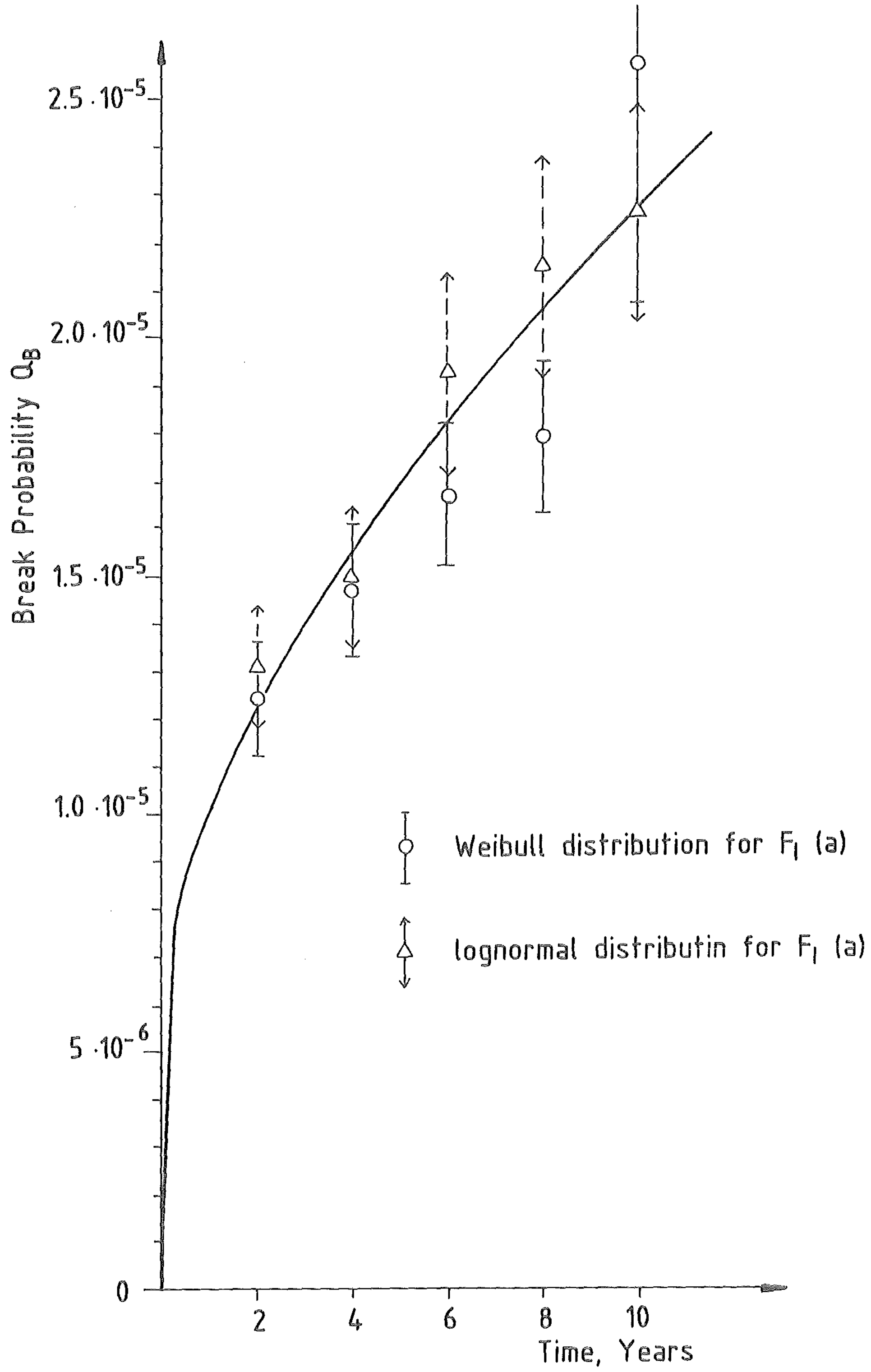

Figure 4.3 Break probability Q_B determined with two different sets of importance sampling distributions, 1000 simulation runs

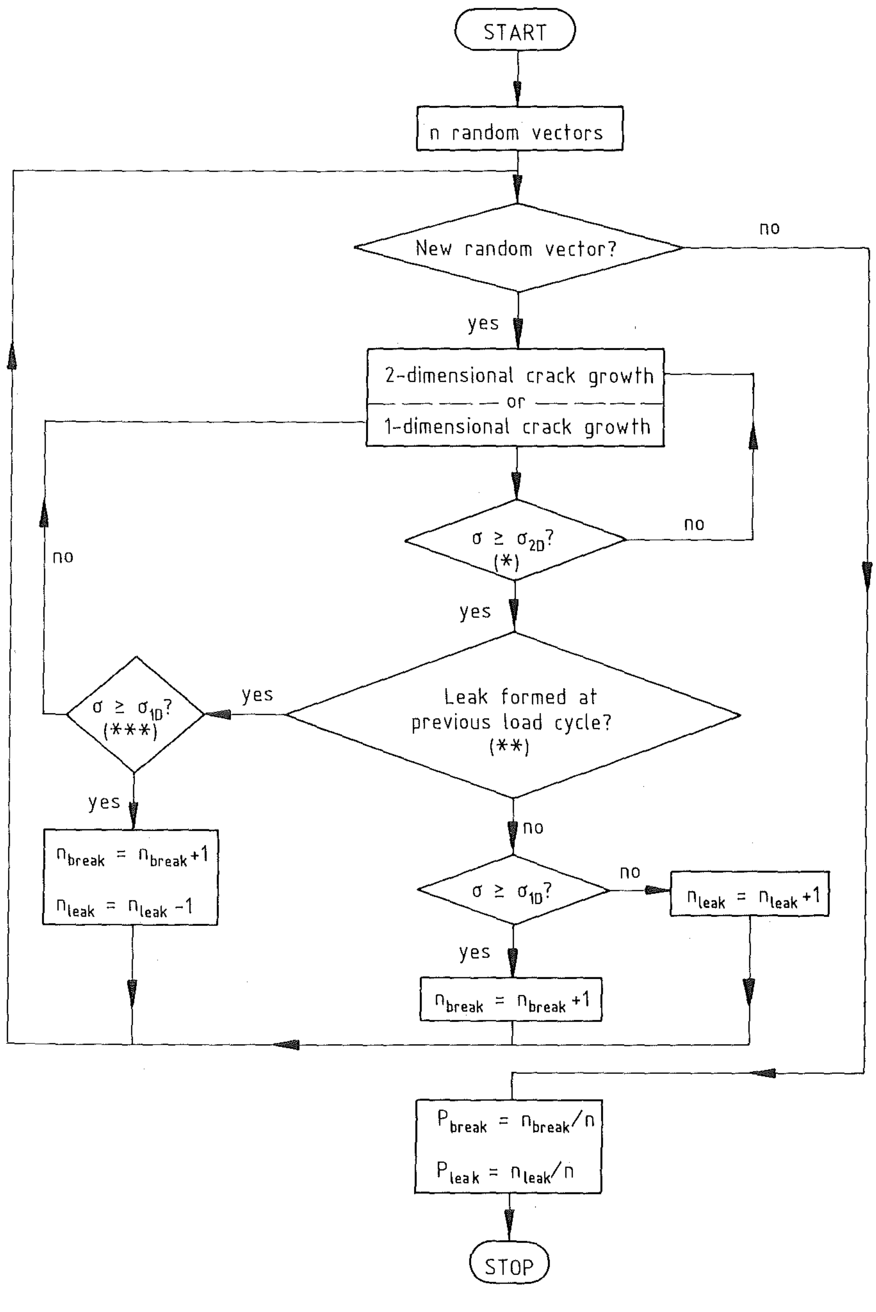

(*) σ_{2D}=0. for through-wall cracks

(**) $\sigma_{2D}<\sigma<\sigma_{1D}$ at previous load cycle

(***) σ_{1D} depends on the load cycle at which the leak was formed

Figure 4.4: Principle of probabilistic leak-before-break analysis without leak detection

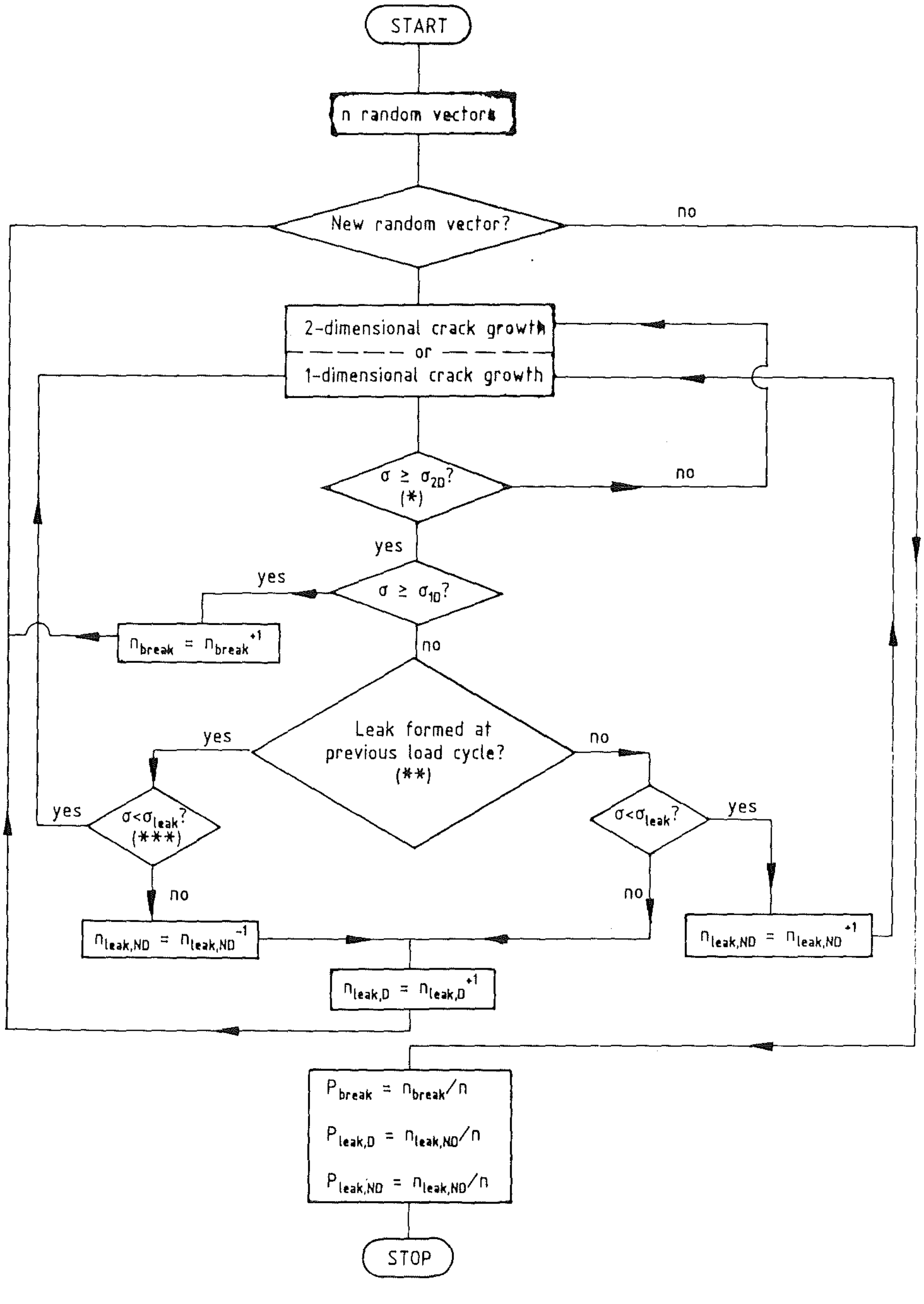

(*) $\sigma_{2D}=0$ for through-wall cracks

(**) $\sigma_{2D}<\sigma<\sigma_{1D}$ at previous load cycle

(***) σ_{leak} depends on the load cycle at which the leak was formed

Figure 4.5 Principle of probabilistic leak-before-break analysis with leak detection

The value of the failure integral eqns. (2.31), (2.32) and corresponding formulae following from eqns. (2.50) - (2.52) specify how many components taken from a sample of size n (= number of simulation runs) contain leaks at a given time and how many have failed by global instability during the period elapsed from start-up.

Without leak detection leaks continue to grow until they cause global instability, i.e. there is a transition between the failure mode leakage and the failure mode breakage. This implies that the leak probability can decrease with increasing number NT of time steps and tends to zero for $NT \to \infty$.

If the benefits of a leak detection system are taken into account, there are three different failure modes: leakage with subsequent detection of the leak, leakage without detection and breakage. Non-detected leaks continue to grow until the leak rate surpasses the critical leak rate of the leak detection system and they are detected. This means that there is a transition from the failure mode "non-detected leak" to the mode "detected leak", but no transition from the mode "leakage" to the mode "breakage". Consequently, $P_{Leak,D}$ and P_{Break} increase with the number of time steps, whereas $P_{Leak,ND}$ tends to zero with $NT \to \infty$.

Figs. 4.6 - 4.7 illustrate how the leak and the break probabilities are influenced by the presence of a leak detection system. From the sample considered (n = 1000), several components fail by global instability caused by unstable growth of leaks as it can be concluded from the dip in Q_{Leak} in Fig. 4.6 and the higher values for Q_{Break} without leak detection in Fig. 4.7. For higher numbers of simulation runs, this dip will, of course, be smeared out.

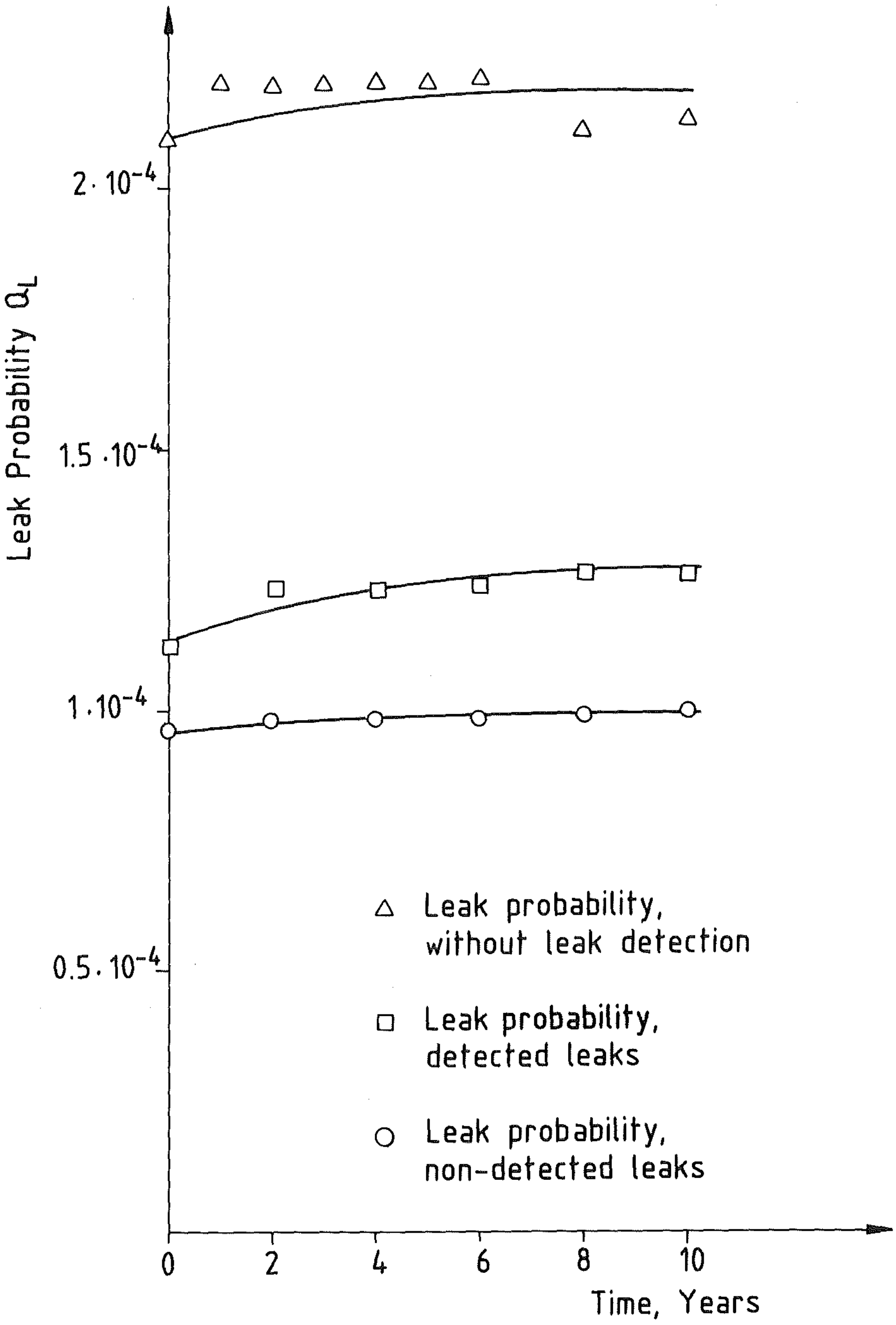

Figure 4.6 Effect of a leak detection system on the leak probability Q_L

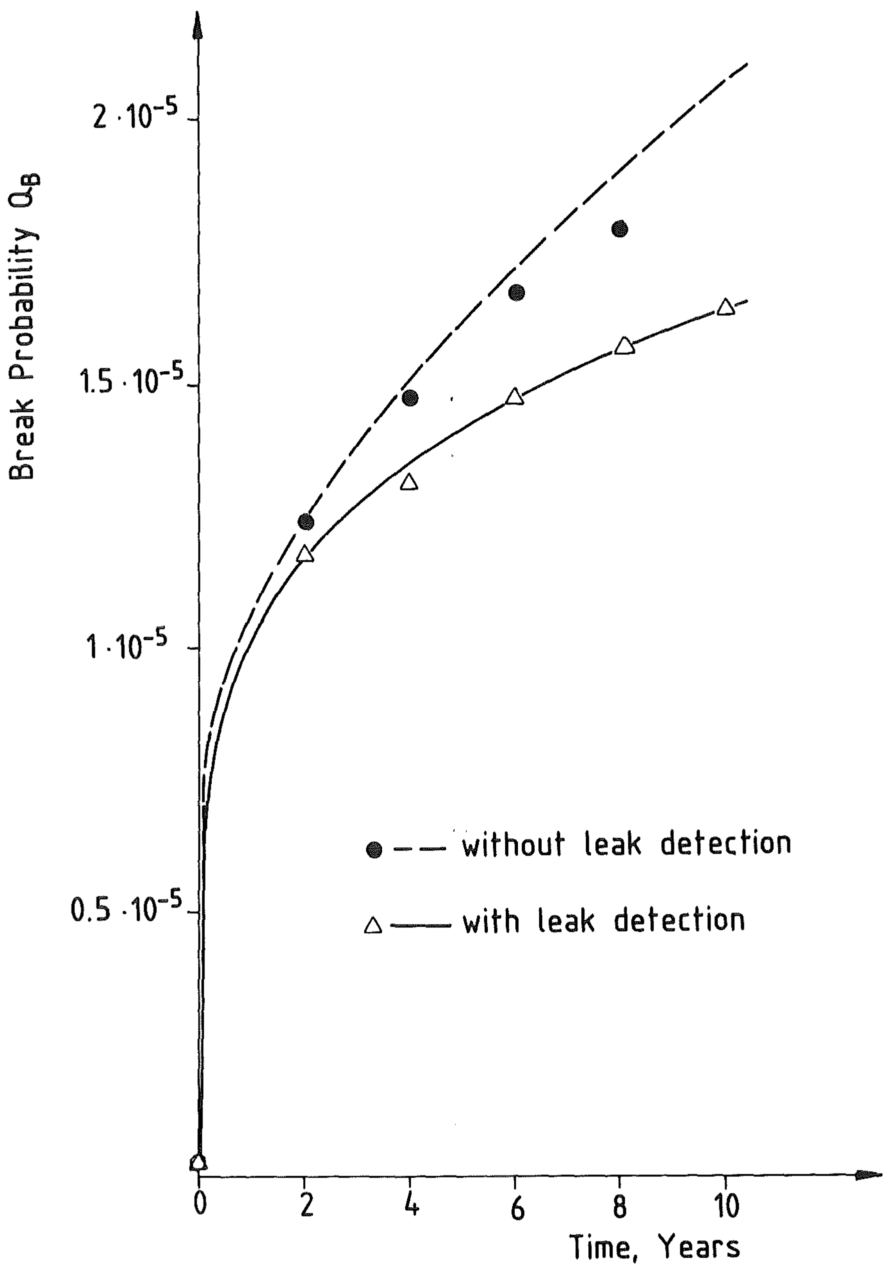

Figure 4.7 Effect of a leak detection system on the break probability Q_B

Concluding Remarks

The PARIS code is a versatile PFM code specifically designed for applications in the nuclear industry. Therefore, special care was taken to incorporate an efficient simulation method for components of high reliability. Previous applications /14, 37/ have shown that failure probabilities of the order of of 10^{-8} or less can be determined with an statistical error of a few per cent.

Nuclear components generally contain welds in which the existence of cracks cannot be excluded. As these cracks normally govern the failure behavior, no effort was made to include crack nucleation. In /14/ it was shown that the failure probabilities following from a rather simplistic crack nucleation model, where crack initation is a Poisson process, can be determined directly from the output of the code.

Another important point in the reliability analysis of nuclear components is the leak-before-break behavior /22/. The code computes leak and break probabilities including the effects of a leak detection system. The leak-before-break criterion is fulfilled in a probabilistic sense if the break probability remains much lower than the leak probability for all PFM models compatible with the data base. The impact on the reliability of other maintenance procedures such as proof tests for pressurized components and non-destructive pre-service and in-service inspections is also taken into account in the code.

Due to its modular structure the PARIS code can easily be adapted to PFM problems different from those considered up to now. For example, crack growth caused by stress corrosion as considered in the PRAISE code /10/ could be taken into account by making minor changes in the input subroutine and the subroutine where the crack growth law is integrated. Consideration of residual stresses as in the PRAISE code would imply a few modifications to be made in the subroutine which determines the stresses for fatigue and failure. More substantial changes are necessary to introduce more sophisticated models for crack initiation and creep. It is planned to develop a second version of the code in the near future which will include these phenomena.

Appendix

A.1 Probability Distributions

All the distributions considered in the code are determined by a maximum of three parameters P1, P2, P3 (= P1(IV), P2(IV), P3(IV) and P1I(IV), P2I(IV), P3I(IV) in the input). User specified lower (UG) and upper (OG) bounds can be taken into account but require additional normalization in subroutine NORMIE. The indices IFLAG (= IVER(IV) and IVERI(IV) in the input routine EINGAB) specifies the distributions as follows:

IFLAG = 1

Exponential distribution

$$f(x) = P1 \exp(- P1 (x-P3)) \tag{A.1}$$

$$F(x) = \exp(- P1 (UG - P3)) - \exp(- P1 (X - P3)).$$

IFLAG = 2

Lognormal distribution

$$f(x) = \frac{1}{\sqrt{2\pi} \cdot P1 \cdot (x - P3)} \cdot \exp\left(- \frac{1}{2}\left(\frac{\ln (x - P3) - \ln P1}{P2}\right)^2\right)$$

(A.2)

$$F(x) = \frac{1}{2}\left[\mathrm{erf}\left(\frac{\ln (x - P3) - \ln P1}{\sqrt{2} \cdot P2}\right) - \mathrm{erf}\left(\frac{\ln (x - P3) - \ln P1}{\sqrt{2} \cdot P2}\right)\right]$$

where

$$\mathrm{erf}(y) = \frac{2}{\sqrt{\pi}} \int_0^y \exp(- t^2)\, dt$$

IFLAG = 3

Normal distribution

$$f(x) = \frac{1}{\sqrt{2\pi}\ P2} \cdot \exp\left(- \frac{1}{2}\left(\frac{x-P1}{P2}\right)^2\right)$$

(A.3)

$$F(x) = \frac{1}{2}\left[\mathrm{erf}\left(\frac{x - P1}{\sqrt{2}\ P2}\right) - \mathrm{erf}\left(\frac{UG - P1}{\sqrt{2}\ P2}\right)\right]$$

IFLAG = 4

Weibull distribution

$$f(x) = \frac{P2}{P1}\left(\frac{x - P3}{P1}\right)^{P2-1} .\exp\left(- \left(\frac{x - P3}{P1}\right)^{P2}\right) \tag{A.4}$$

$$F(x) = \exp\left(-\left(\frac{UG - P3}{P1}\right)^{P2}\right) - \exp\left(-\left(\frac{x - P3}{P1}\right)^{P2}\right)$$

IFLAG = 5

Gamma distribution

$$f(x) = \frac{P1 \quad (P1\,(x-P3))^{P2-1}}{\Gamma\,(P2)} \cdot \exp\,(-\,P1 \cdot (x - P3)) \qquad \text{(A.5)}$$

$$F(x) = \int_{UG}^{x} f(x)\,dx \qquad \text{(numerical integration)}$$

IFLAG = 6

Uniform distribution

$$f(x) = \frac{1}{P2 - P1} \qquad \text{(A.6)}$$

$$F(x) = \frac{1}{P2 - P1}\,(x - UG)$$

IFLAG = 7

Gumbel extreme value distribution

$$f(x) = \frac{1}{P2} \exp\left(-\frac{x - P1}{P2} - \exp\left(-\frac{x - P1}{P2}\right)\right) \qquad \text{(A.7)}$$

$$F(x) = \exp\left(-\exp\left(-\frac{x - P1}{P2}\right)\right) - \exp\left(-\exp\left(-\frac{UG - P1}{P2}\right)\right)$$

IFLAG = 8 constant value

$$f(x) = \delta(x - P1) \qquad \text{(A.8)}$$

where $\delta(y)$ is Dirac's δ-function and

$$F(x) = \Theta(x - P1)$$

where $\Theta(y)$ is the step function.

A.2 Random Number Generators

The IMSL-library /26/ contains several random number generators for various types of distribution. For the sake of simplicity only a generator for uniformly distributed random numbers, called GGUBFS, a generator for normally distributed random numbers (GGNQF) and a generator for gamma distributed random numbers (GGAMR) are used. All other random numbers z can be generated by simple transformations as follows:

IFLAG = 1, exponential distribution:

$$\xi = \mathrm{GGUBFS(DSEED)}$$

$$z = -\frac{1}{P1}\cdot \ln\,(\exp(-P1\cdot UG) - \xi\cdot(\exp(-P1\cdot UG)-\exp(P1\cdot OG))) \quad (A.9)$$

where P3 = UG was assumed.

IFLAG = 2, lognormal distribution:

$$\xi = \mathrm{GGNQF(DSEED)}$$

$$z = \exp(\xi\cdot P2)\cdot P1 + P3 \quad (A.10)$$

IFLAG = 3, normal distribution:

$$\xi = \mathrm{GGNQF(DSEED)}$$

$$z = \xi\cdot P2 + P1 \quad (A.11)$$

IFLAG = 4, Weibull distribution:

$$\xi = \mathrm{GGUBFS(DSEED)}$$

$$z = P1\cdot(-\ln(y_1+\xi\cdot(y_2- y_1)))^{1/P2} + P3 \quad (A.12)$$

with

$$y_1 = \exp\left(-\left(\frac{UG}{P1}\right)^{P2}\right) \quad (A.13)$$

$$y_2 = \exp\left(-\left(\frac{OG}{P1}\right)^{P2}\right)$$

IFLAG = 5, gamma distribution: random numbers directly generated by GGAMR

IFLAG = 6, uniform distribution

$$\xi = \mathrm{GGUBFS(DSEED)}$$

$$z = \xi \cdot (P2 - P1) + P1 \qquad (A.14)$$

IFLAG = 7, Gumbel extreme value distribution

$$\xi = \mathrm{GGUBFS(DSEED)}$$

$$z = - \ln (- \ln (y_1 + \xi \cdot (y_2 - y_1))) \cdot P2 + P1 \qquad (A.15)$$

$$y_1 = \exp (- \exp (- \frac{UG - P1}{P2})) \qquad y_2 = \exp (- \exp (- \frac{OG - P1}{P2})) \qquad (A.16)$$

IFLAG = 8, constant value

$$z = P1 \qquad (A.17)$$

A suitable starting number has to be assigned to the starting value DSEED of the random number generators. The PARIS code uses

$$\mathrm{DSEED} = 123457. \qquad (A.18)$$

which is recommended in /26/. All random numbers z are supposed to lie in the interval spanned by the lower bound UG and the upper bound OG. In cases where the random number generator yields unbounded values for z, all numbers not contained in (UG, OG) are rejected.

A.3 Stress Intensity Factors

Subroutines TAKA and TAKB contain stress intensity factors for a variety of one- and two-dimensional cracks. With the notation

$$K_A = \sigma \cdot \sqrt{\pi a} \cdot Y_A \tag{A.19}$$

and

$$K_B = \sigma \cdot \sqrt{\pi a} \cdot Y_B \tag{A.20}$$

where $Y_B = 0$ for one-dimensional cracks, the index IK selects one of the following crack models:

IK = 1 Center cracked plate subjected to tension (Fig. A.1, /38/)

$$Y_A = \frac{1}{\sqrt{1 - a/w}} \cdot (1 - \frac{a}{2w} + 0.326 \left(\frac{a}{w}\right)^2) \tag{A.21}$$

where 2w is the width of the plate.

IK = 2: Three-point-bending specimen (Fig. A.2, /38/)

$$Y_A = \frac{1}{\sqrt{\pi}} \cdot \frac{1.99 - \frac{a}{t} \cdot \left(1 - \frac{a}{t}\right) \cdot \left(2.15 - 3.93 \cdot \frac{a}{t} + 2.7 \left(\frac{a}{t}\right)^2\right)}{\left(1 + 2\frac{a}{t}\right) \cdot \left(1 - \frac{a}{t}\right)^{1.5}} \tag{A.22}$$

where t is the thickness of the specimen.

IK = 3: Longitudinally cracked pipe subjected to internal pressure (Fig. A.3, /39/)

$$Y_A = (1 + 0.3801\ \lambda^2 - 0.00124\ \lambda^4)^{1/2} \tag{A.23}$$

with

$$\lambda = \frac{a}{\sqrt{R_i t}} (12 \cdot (1 - \nu^2))^{0.25} \tag{A.24}$$

where R_i is the inner radius and t the wall thickness.

IK = 4 Circumferentially cracked pipe subjected to tension (Fig. A.4, /40/)

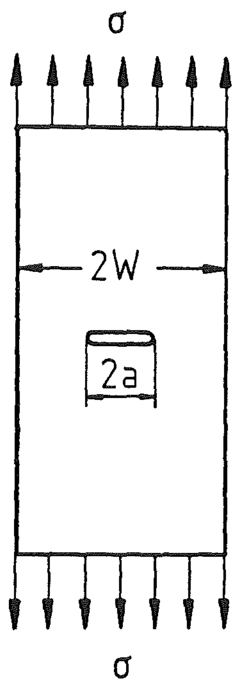

Figure A.1 Center cracked plate

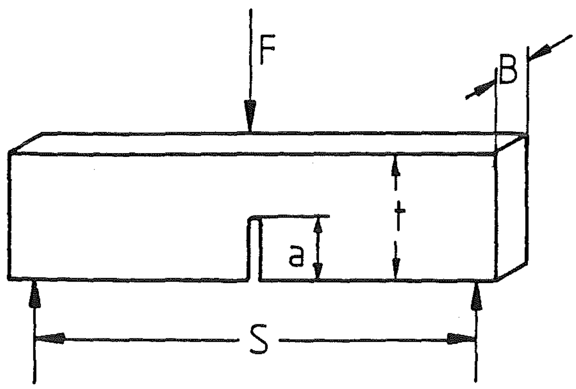

Figure A.2 Three-point bending specimen

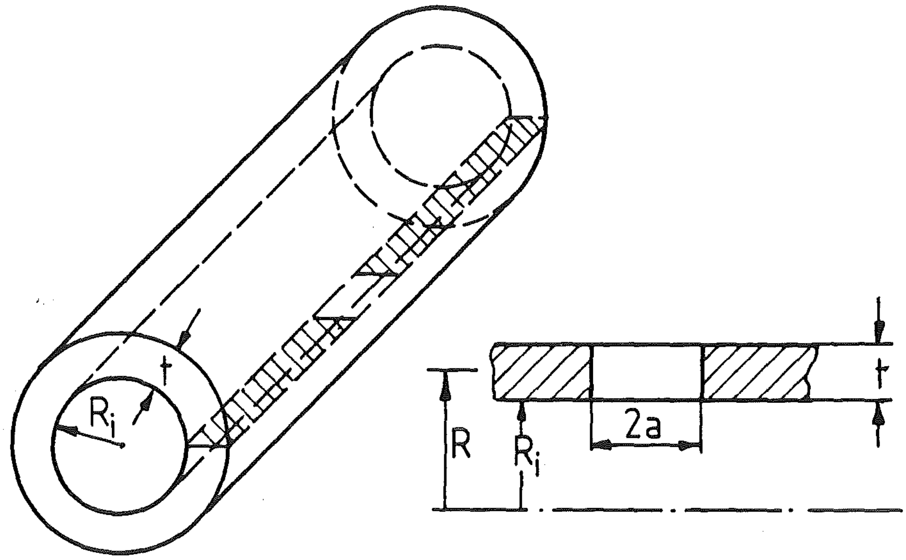

Figure A.3 Pipe with a through-wall longitudinal crack

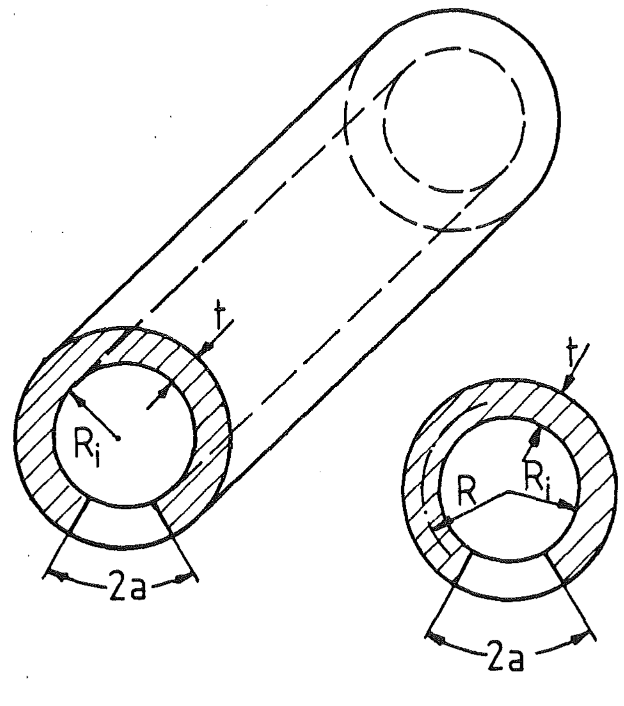

Figure A.4 Pipe with a through-wall circumferential crack

$$Y_A = \left[\frac{\lambda}{2\pi} \cdot (g\ (\alpha) + \frac{2\pi\ C^2}{\lambda} - 2\sqrt{2}) \right]^{1/2} \tag{A.25}$$

with

$$g\ (\alpha) = 2\sqrt{2} \left[1 + \frac{1 - \alpha \cot \alpha}{2\alpha \cot \alpha + \sqrt{2}\ \alpha \cot \frac{\pi - \alpha}{\sqrt{2}}} \right]^2$$

and

$$C = \begin{cases} 1 + \frac{\pi}{64} \lambda^2 - 0.00366\ \lambda^3 & \text{for } \lambda \leq 2 \\ \left(\frac{\sqrt{2}}{\pi} \lambda \right)^{1/2} + \left(\frac{0.258}{\lambda} \right)^{0.885} & \text{for } \lambda > 2 \end{cases}$$

IK = 5 Circumferentially cracked pipe with a linear stress gradient across the wall (Fig. A.4, /41/)

$$Y_A = (1 + 0.0222\ \lambda + 0.0424\ \lambda^2 - 0.0057\ \lambda^3 + 0.000241\ \lambda^4)\ (1 + \frac{\sigma_b}{2\sigma}) \tag{A.26}$$

where

$$\sigma = \frac{\sigma_i + \sigma_0}{2} \tag{A.27}$$

is the arithmetic mean of the applied stresses at the outer (σ_o) and the inner (σ_i) surfaces of the pipe, and

$$\sigma_b = \frac{\sigma_0 - \sigma_i}{2} \tag{A.28}$$

is the relative bending component of the stress.

IK = 6 Longitudinally cracked pipe with a linear stress gradient across the wall (Fig. A.3, /42/)

$$Y_A = (0.614 + 0.481\ \lambda + 0.386\ \exp\ (-1.25\ \lambda)) \cdot \left(1 + \frac{\sigma_b}{2\sigma}\right) \tag{A.29}$$

IK = 7 User option for a one-dimensional crack

IK = 8 Plate containing a semi-elliptical surface crack subjected to tension (Fig. A.5, /43/)

(Fig. A.5, /43/)

$$Y_A = \frac{F}{\sqrt{Q}}, \quad Y_B = \frac{F}{\sqrt{Q}} \cdot f_B \tag{A.30}$$

with

$$Q = 1 + 1.464 \left(\frac{a}{c}\right)^{1.65} \tag{A.31}$$

and

$$F = M_1 + M_2 \cdot \left(\frac{a}{t}\right)^2 + M_3 \cdot \left(\frac{a}{t}\right)^4 \tag{A.32}$$

$$M_1 = 1.13 - 0.09 \frac{a}{c}$$

$$M_2 = -0.54 + \frac{0.89}{0.2 + a/c}$$

$$M_3 = 0.5 - \frac{1}{0.65 + a/c} + 14 \cdot \left(1 - \frac{a}{c}\right)^{24}$$

The correction factor f_B is given by:

$$f_B = \sqrt{\frac{a}{c}} \left(1.1 + 0.35 \left(\frac{a}{t}\right)^2\right) \tag{A.33}$$

IK = 9 Plate containing a semi-elliptical surface crack subjected to combined tension and bending (Fig. A.5, /43/)

$$Y_A = \frac{F}{\sqrt{Q}} \cdot \left(1 + \frac{\sigma_b}{\sigma} \cdot H_A\right), \tag{A.34}$$

$$Y_B = \frac{F}{\sqrt{Q}} \cdot \left(1 + \frac{\sigma_b}{\sigma} \cdot H_B\right) \cdot f_B$$

where F, Q, f_B are defined in eqns. (A.31) - (A.33) σ is the membrane stress, and σ_b is the bending stress, and H_A, H_B are determined from:

$$H_A = 1 + G_1 \cdot \frac{a}{t} + G_2 \cdot \left(\frac{a}{t}\right)^2$$

$$G_1 = -1.22 - 0.12 \frac{a}{c} \tag{A.35}$$

$$G_2 = 0.55 - 1.05 \cdot \left(\frac{a}{c}\right)^{0.75} + 0.47 \cdot \left(\frac{a}{c}\right)^{1.5}$$

and

$$H_B = 1 - \left(0.34 + 0.11 \frac{a}{c}\right) \cdot \frac{a}{t} \tag{A.36}$$

IK = 10 Pipe containing an internal longitudinal semi-elliptical surface crack subjected to internal pressure (Fig. A.6, /44/)

$$Y_A = \frac{F}{\sqrt{Q}} \; f_c \cdot 0.97, \tag{A.37}$$

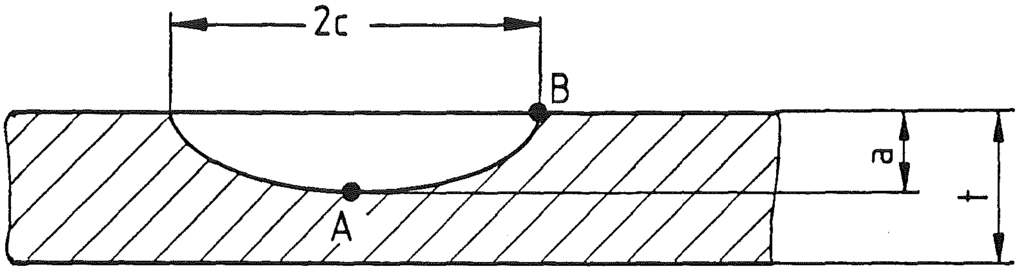

Figure A.5 Semi-elliptical surface crack in a plate

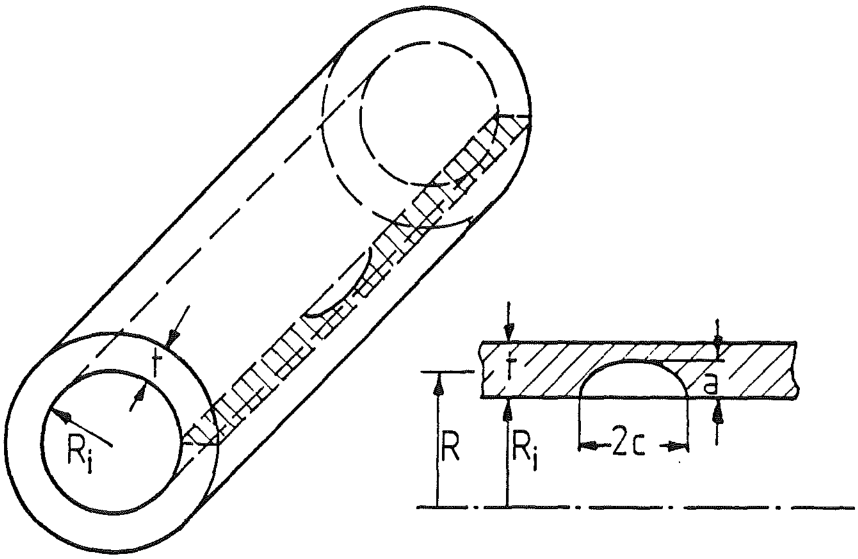

Figure A.6 Semi-elliptical longitudinal surface crack in a pipe

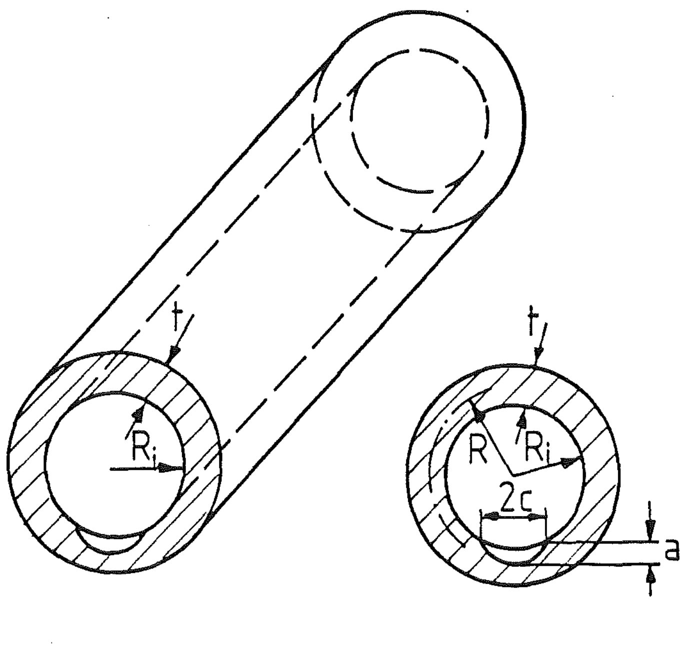

Figure A.7 Semi-elliptical circumferential surface crack in a pipe

$$Y_B = \frac{F}{\sqrt{Q}} f_B \cdot f_c \cdot 0.97$$

where F, Q, f_B are given in eqns. (A.31) - (A.33) and f_c is defined as:

$$f_c = \left(\frac{R_0^2 + R_i^2}{R_0^2 - R_i^2} + 1 - 0.5 \sqrt{\frac{a}{t}} \right) \cdot \frac{t}{R_i} \qquad (A.38)$$

with R_o denoting the outer radius and R_i the inner radius of the pipe.

IK = 11 Pipe containing an internal longitudinal semi-elliptical surface crack subjected to internal pressure (Fig. A.6, /30/)

$$Y_A = M_m \cdot M_R \cdot \frac{1}{\sqrt{Q}}$$

$$Y_B = Y_A \cdot \sqrt{\frac{a}{c}} \qquad (A.39)$$

with

$$M_m = 1.1 + 5.2 \cdot \left(\frac{1}{32} \right)^{a/c} \cdot \left(\frac{a}{t} \right)^{1.8+a/c}$$

$$M_R = \frac{A_m - a/t}{A_m \, (1 - a/t)} \qquad (A.40)$$

$$A_m = \sqrt{1 + 1.61 \, c^2/Rt}$$

where

$$R = \frac{1}{2} (R_i + R_0)$$

is the mean radius of the pipe.

IK = 12 Pipe containing an internal circumferential semi-elliptical surface crack subjected to tension (Fig. A.7, /10/)

$$Y_A = \frac{1.15}{\sqrt{1-a/t}} \cdot \left(H_0 + H_1 \cdot \frac{a}{t} + H_2 \cdot \left(\frac{a}{t}\right)^2 + H_3 \cdot \left(\frac{a}{t}\right)^3 \right) \cdot \frac{1.}{\sqrt{\pi}}$$

$$Y_B = \frac{1.15}{\sqrt{1-a/t}} \cdot \left(I_0 + I_i \cdot \frac{a}{t} + I_2 \cdot \left(\frac{a}{t}\right)^2 + I_3 \cdot \left(\frac{a}{t}\right)^3 \right) \cdot \frac{1.}{\sqrt{\pi}} \qquad (A.41)$$

$$H_0 = 1.44 - 0.343 \frac{a}{c} - 0.404 \left(\frac{a}{c}\right)^2 + 0.293 \left(\frac{a}{c}\right)^3$$

$$H_1 = -0.682 - 0.423 \frac{a}{c} - 0.497 \left(\frac{a}{c}\right)^2 + 0.970 \left(\frac{a}{c}\right)^3$$

$$H_2 = 0.0366 + 11.80 \frac{a}{c} - 20.73 \left(\frac{a}{c}\right)^2 + 9.69 \left(\frac{a}{c}\right)^3$$

$$H_3 = 0.426 - 15.83 \frac{a}{c} + 29.54 \left(\frac{a}{c}\right)^2 - 15.04 \left(\frac{a}{c}\right)^3$$

$$I_0 = 0.979 + 0.202 \frac{a}{c} - 0.248 \left(\frac{a}{c}\right)^2 + 0.055 \left(\frac{a}{c}\right)^3$$

$$I_1 = 1.06 - 6.69 \frac{a}{c} + 9.22 \left(\frac{a}{c}\right)^2 - 4.29 \left(\frac{a}{c}\right)^3$$

$$I_2 = - 2.75 + 21.82 \frac{a}{c} - 36.22 \left(\frac{a}{c}\right)^2 + 18.61 \left(\frac{a}{c}\right)^3$$

$$I_3 = 1.43 - 17.71 \frac{a}{c} + 31.19 \left(\frac{a}{c}\right)^2 - 16.48 \left(\frac{a}{c}\right)^3$$

IK = 13 Pipe containing an external circumferential surface crack with a linear stress gradient across the wall (Fig. A.7, /41/, /43/)

$$Y_A = \frac{F}{\sqrt{Q}} \cdot \left(1 + \frac{\sigma_b}{\sigma} \cdot H_A\right) \cdot f_D \,,$$

$$Y_B = \frac{F}{\sqrt{Q}} \cdot \left(1 + \frac{\sigma_b}{\sigma} \cdot H_B\right) \cdot f_B \cdot f_D \qquad \text{(A.42)}$$

where F, Q, f_B, H_A, H_B are defined in eqns. (A.31) – (A.33), (A.35), (A.36), σ, σ_b follow from eqns. (A.27), (A.28) and f_D is equal to:

$$f_D = (B_m - 1) \cdot \frac{a}{t} + 1 \qquad \text{(A.43)}$$

with $B_m = 1 + 0.0222\,\lambda_s + 0.0424\,\lambda_s^2 - 0.0057\,\lambda_s^3 - 0.000241\,\lambda_s^4$

and

$$\lambda_s = \frac{c}{\sqrt{R_i\, t}} \cdot (12 \quad (1 - \nu^2))^{0.25} \qquad \text{(A.44)}$$

IK = 14 Pipe containing an external longitudinal surface crack with a linear stress gradient across the wall (Fig. A.6, /42/, /43/)

$$Y_A = \frac{F}{\sqrt{Q}} \cdot \left(1 + \frac{\sigma_b}{\sigma} H_A\right) \cdot f_L \,,$$

$$\text{(A.45)}$$

$$Y_B = \frac{F}{\sqrt{Q}} \cdot \left(1 + \frac{\sigma_b}{\sigma} H_B\right) \cdot f_L$$

where F, Q, f_B, H_A, H_B are defined in eqns. (A.31) – (A.33), (A.35), (A.36), σ, σ_b are given in eqns. (A.27), (A.28) and f_L follows from:

$$f_L = (A_m - 1)\frac{a}{t} + 1 \quad \text{(A.46)}$$

with

$$A_m = 0.614 + 0.481\,\lambda_s + 0.386 \cdot \exp(-1.25\,\lambda_s)$$

and λ_S as in eqn. (A.44).

IK = 15 User option for two-dimensional cracks.

A.4 Plastic Limit Loads

Plastic limit loads are determined in subroutine PG. Depending on the value of the index IP the limit load

$$\sigma_L = \sigma_f \cdot M \tag{A.47}$$

where σ_f is the flow stress, is determined by one of the following relations:

IP = 1 Center cracked plate subjected to tension (Fig. A.1, /45/)

$$M = 1 - \frac{a}{w} \tag{A.48}$$

where 2w is the width of the plate.

IP = 2 Three-point bending specimen (Fig. A.2, /45/)

$$M = \frac{3}{2} \left(1 - \frac{a}{w}\right)^2 \tag{A.49}$$

IP = 3 Longitudinally cracked pipe subjected to internal pressure with a linear stress gradient across the wall (Fig. A.3, /39/)

$$M = (1 + 0.3801\ \lambda^2 - 0.00124\ \lambda^4)^{-1/2} - \frac{\sigma_b}{2\sigma_f} \tag{A.50}$$

where λ follows from eqn. (A.24) and σ_b from eqns. (A.27), (A.28).

IP = 4 Longitudinally cracked pipe subjected to internal pressure (Fig. A.3, /46/)

$$M = \begin{cases} \dfrac{1}{1 + \lambda_1^2} + 0.12 & \lambda_1 \geq 1 \\[2ex] \dfrac{\sqrt{1 + 8\ \lambda_1^2} - 1}{4\ \lambda_1^2} + 0.12\ \lambda_1 & \lambda_1 < 1 \end{cases} \tag{A.51}$$

with

$$\lambda_1 = c/\sqrt{R_i\ t} \tag{A.52}$$

IP = 5 Circumferentially cracked pipe with a linear stress gradient across the wall (Fig. A.4, /41/)

$$M = (1 + 0.0222\ \lambda + 0.0424\ \lambda^2 - 0.0057\ \lambda^3 + 0.000241\ \lambda^4)^{-1} - \frac{\sigma_b}{2\sigma_f} \tag{A.53}$$

where λ is defined in (A.24) and σ_b in eqns. (A.27), (A.28).

IP = 6 Circumferentially cracked pipe subjected to tension (Fig. A.4, /10/)

$$M = 1 - \frac{a}{\pi R} \tag{A.54}$$

where R is the mean radius of the pipe.

IP = 7 Longitudinally cracked pipe with a linear stress gradient across the wall (Fig. A.3, /42/)

$$M = (0.614 + 0.481\,\lambda + 0.386 \cdot \exp\,(-1.25\,\lambda))^{-1} - \frac{\sigma_b}{2\sigma_f} \tag{A.55}$$

IP = 8 User option

IP = 9 Plate containing a semi-elliptical surface crack subjected to tension (Fig. A.5, /45/)

$$M = 1 - \frac{a}{t} \; \frac{(1 + 2(\frac{c}{t})^2)^{1/2} - 1}{(1 + 2\,(\frac{c}{t})^2)^{1/2} - \frac{a}{t}} \tag{A.56}$$

IP = 10 Plate containing a semi-elliptical surface crack subjected to tension (Fig. A.5, /47/)

$$M = (1 - P_1 \cdot P_2) \quad (1 - (\frac{a}{t})^{1.4}) \tag{A.57}$$

with

$$P_1 = -\,1.907 \cdot \frac{a}{t} + 1.515 \cdot (\frac{a}{c})^{0.166} \cdot (\frac{a}{t})^2 - 21.52 \cdot (\frac{a}{c})^{2.142} \cdot (\frac{a}{t})^3 + 0.342 \cdot (\frac{a}{t})^4$$

$$P_2 = -\,0.74 + 3.859\,(\frac{a}{c}) - 3.825\,(\frac{a}{c})^2 - 2.89\,(\frac{a}{c})^3 + 4.356\,(\frac{a}{c})^4$$

σ_f in eqn. (A.37) is supposed to be

$$\sigma_f = 1.15\,R_p \tag{A.58}$$

if eqn. (A.57) is used to determine the plastic limit load.

IP = 11 Plate containing a semi-elliptical surface crack subjected to tension (Fig. A.5, /25/)

$$M = 1 - \frac{\pi ac}{2t\cdot(t+2c)} \tag{A.59}$$

IP = 12 Plate containing a semi-elliptical surface crack subjected to combined tension and bending (Fig. A.5, /25/)

$$M = - \frac{a}{t} + \left\{ 1 + 2\left(\frac{a}{t}\right)^2 - 2\cdot\frac{a}{t} - \frac{\sigma_b}{2\sigma_f} \right\}^{1/2} \tag{A.60}$$

where σ_b is the bending stress.

IP = 13 Pipe containing an external longitudinal surface crack subjected to internal pressure (Fig. A.6, /39/).

$$M = \frac{C_m - \frac{a}{t}}{C_m\cdot(1 - \frac{a}{t})} \tag{A.61}$$

with

$$C_m = (1 + 0.3801\cdot\lambda_s^{\,2} - 0.00124\cdot\lambda_s^{\,4})^{1/2} \tag{A.62}$$

and λ_S as in eqn. (A.44).

IP = 14 Pipe containing an internal circumferential surface crack subjected to tension (Fig. A.7, /10/)

$$M = 1 - \frac{ac\cdot(2R_i + a)}{\pi R_i t\cdot(2R_i + t)} \tag{A.63}$$

IP = 15 User option for a two-dimensional crack.

References

/1/ G.O. Johnston, A review of probabilistic fracture mechanics literature, Reliability Engineering, 3, 6(1982) 423-448.

/2/ C. Sundararajan, Probabilistic assessment of pressure vessel and piping reliability, J. Pressure Vessel Technology, Trans. ASME, 108 (1986) 1-13.

/3/ H.W. Bargmann, Prediction of pressure vessel failure: a critical review of the probabilistic approach, Theoretical and Applied Fracture Mechanics, 5 (1986) 1-16.

/4/ J.W. Provan (Editor), Probabilistic Fracture Mechanics and Reliability, M. Nijhoff Publ., 1986.

/5/ R.W. Gates, The relationship between load factors and failure probabilities determined from a full elasto-plastic probabilistic fracture mechanics analysis, Int. J. Pressure Vessels and Piping 13 (1983) 155-167.

/6/ W.E. Vesely, E.K. Lynn, F.F. Goldberg, The OCTAVIA computer code: PWR reactor pressure vessel failure probabilities due to operationally caused pressure transients, Report NUREG-0258, U.S. Nuclear Regulatory Commission, Washington 1978.

/7/ F.A. Simonen, K.I. Johnson, A. Liebetrau, D.W. Engel, E.P. Simonen, VISA II - a computer code for predicting the probability of reactor pressure vessel failure, Report NUREG/CR-4486, PNL-5725, Pacific Northwest Laboratory, Richland, Washington 1986.

/8/ R.D. Cheverton, D.G. Ball, OCA-P, A determinstic and probabilistic fracture mechanics code for application to pressure vessels, NUREG/CR-3618, ORNL-5991, Oak Ridge National Laboratories 1984.

/9/ J. Dufresne, A.C. Lucia, J. Grandemange, A. Pellisier-Tanon, Etude probabiliste de la rupture de cuve de reacteurs a eau sous pression, Report EUR 8682 F, Joint Research Centre, Ispra, Italy.

/10/ D.O. Harris, E.Y. Lim, D.D. Dedhia, Probability of pipe fracture in the primary coolant loop of a PWR, probabilistic fracture mechanics analysis, Report NUREG/CR-2189. Vol. 5, US Nuclear Regulatory Commission 1981.

/11/ U. Bourgund, C.G. Bucher, Importance sampling procedure using design points (ISPUD) - a user's manual, Report 8 - 86, Institute of Engineering Mechanics, University of Innsbruck, Austria, 1986.

/12/ J.M. Hammersley, D.C. Handscomb, Monte Carlo Methods, Chapman and Hall, London 1979.

/13/ J. Spanier, An analytic approach to variance reduction, SIAM J. on Applied Mathematics 18 (1970) 172-190.

/14/ J. Theodoropoulos, A. Brückner, Probabilistische Analyse eines Rohrkrümmers im SNR 300, to appear as KfK-Report, Nuclear Research Centre Karlsruhe, 1987.

/15/ M. Mazumdar, Importance sampling in reliability estimation, in: Reliability and Fault Tree Analysis, Philadelphia 1975, pp. 153 - 163.

/16/ D.O. Harris, A means of assessing the effects of NDE on the reliability of cyclically load structures, Materials Evaluation (July 1977) 57 - 65.

/17/ Y.K. Lin, J.N. Yang, A stochastic theory of fatigue crack propagation, AIAA Journal 23, 1(1985) 117 - 124.

/18/ J.N. Yang, G.C. Salivar, C.G. Annis, Statistics of crack growth in engine materials - Vol. 1: Constant amplitude fatigue crack growth at elevated temperatures, Report AFWAL-TR-82-4040, Pratt & Whitney Aircraft Group, West Palm Beach, Florida 1982.

/19/ J.L. Bogdanoff, F. Kozin, Probabilistic models of fatigue crack growth, Engineering Fracture Mechanics 20, 2(1984) 255-270.

/20/ O. Ditlevsen, Random fatigue crack growth - a first passage problem, Engineering Fracture Mechanics 22 (1985) 467-477.

/21/ D.O. Harris, A means of assessing the effects of periodic proof testing and NDE on the reliability of cyclic loaded structures, J. Pressure Vessel Technology, Trans. ASME, 100 (1978) 150-157.

/22/ D. Munz (Editor) Leck-vor-Bruch-Verhalten druckbeaufschlagter Komponenten, VDI-Reihe, 18, 14 (1984).

/23/ A. Brückner, D. Munz, The effect of curve fitting on the prediction of failure probabilities from the scatter in crack geometry and fracture toughness, Reliability Engineering 5 (1983) 139-156.

/24/ A. Brückner, Numerical methods in probabilistic fracture mechanics, Chapter 8 in /4/.

/25/ R. Harrison, K. Loosemore, I. Milne, A.R. Dowling, Assessment of the integrity of structures containing defects, CEGB/R/H/6, Rev. 2, 1980.

/26/ IMSL Library, Edition 9.2, 1984.

/27/ C. Paris, The fracture mechanics approach to fatigue, in: Fatigue, Proc. 10th Sajamore Army Materials Research Conf., Syracuse, New York 1964, 107-138.

/28/ K. Walker, The effect of stress ratio during crack propagation and fatigue for 2024-T3 and 7075-T6 aluminum alloy, ASTM STP 462, 1-13, American Society for Testing Materials 1970.

/29/ R.G. Forman, V.E. Kearney, R.M. Engle, Numerical analysis of crack propagation in cyclic-loaded structures, J. Basis Engineering, Trans. ASME, Series D, 89 (1967) 459-470.

/30/ ASME Boiler and Pressure Vessel Code, Section XI.

/31/ R. Schäfer, G.I. Schueller, P. Kafka, Probabilistische Untersuchung des Rißfortschrittsverhaltens von Reaktorkomponenten, IABG, Report TF-1605, Ottobrunn, Germany 1984.

/32/ W. Marshall, An assessment of the integritiy of PWR pressure vessels, Report of a study group chaired by Dr. W. Marshall, UKAEA 1976.

/33/ F.L. Becker, et al., Integration of NDE reliability and fracture mechanics, Report NUREG/CR-1696, PNL-3469, Pacific North-West Laboratories 1981.

/34/ A. Brückner, T. Schmidt, J. Theodoropoulos, Comparison between the PRAISE code and the PARIS code, to be published.

/35/ O. Ditlevsen, Principle of normal tail approximation, J. Engineering Mechanics, ASCE, 107 (1981) 1191 - 1208.

/36/ A. Harbitz, Efficient and accurate probability of fracture calculation by use of the importance sampling technique, 4th Int. Conf. Applications of Statistics and Probability in Soil and Structural Engineering, Florence, Italy 1983.

/37/ R. Häberer, A. Brückner, D. Munz, Zuverlässigkeitsberechnung mit Hilfe der probabilistischen Bruchmechanik am Beispiel des Sicherheitseinschlusses von Druckwasserreaktoren, Teil I - III, KfK Reports No. 3458, No. 3546, No. 3561, Nuclear Research Center Karlsruhe, West Germany 1983

/38/ H. Tada, P.C. Paris, G.R. Irwin, The Stress Analysis of Cracks Handbook (2nd. Ed.), Paris Prod. Inc., St. Louis, Missouri 1985.

/39/ J.F. Kiefner, W.A. Maxey, R.J. Eiber, A.R. Duffy, Failure stress levels of flaws in pressurized cylinders, ASTM STP 526, 461-481, American Society for Testing Materials 1973.

/40/ R.G. Forman, J.C. Hickman, V. Shivakumar, Stress intensity factors for circumferential through-wall cracks in hollow cylinders subjected to combined tension and bending loads, Engineering Fracture Mechanics, 21 (1985) 563-571.

/41/ F. Erdogan, Theoretical and experimental study of fracture in pipelines containing an initial surface flaw, Report DOT-RSPA-DMA-50/83/3, National Technical Information Service, Springfield, Virginia 1982.

/42/ F. Erdogan, M. Ratwani, Fracture initiation and propagation in a cylindrical shell containing an initial surface flaw, Nuclear Engineering and Design, 27 (1974) 14-29.

/43/ J.C. Newman, I.S. Raju, An empirical stress intensity factor equation for the surface crack, Engineering Fracture Mechanics, 15 (1981) 185-192.

/44/ J.C. Newman, I.S. Raju, Stress intensity factor for internal surface cracks in cylindrical pressure vessels, J. Pressure Technology, Trans. ASME, 102 (1980) 342-346.

/45/ G.G. Chell, Elastic-plastic fracture mechanics, in: Development in Fracture Mechanics, Vol. I, ed. by G.G. Chell, Applied Science Publ., London 1979.

/46/ R. Kitching, J.K. Davies, S.S. Gill, Limit pressure for cylindrical shells with unreinforced openings of various shapes, J. Mechanical Engineering Science 12 (1970) 313-330.

/47/ C. Mattheck, P. Morawietz, D. Munz, B. Wolf, Ligament yielding of a plate with semi-elliptical surface cracks under uniform tension, Int. J. Pressure Vessels and Piping 16 (1984), 131-143.